Studies on the molecular mechanisms of mouse germ cell development

マウス生殖細胞の発生過程における分子機構に関する研究

山口　泰華

奈良先端科学技術大学院大学

バイオサイエンス研究科　　分子発生生物学講座

（高橋　淑子教授）

TABLE OF CONTENTS

Chapter I ABSTRACT

Germ cells are specialized for transmitting genetic information to the next generation. A unique property of germ cells which sets them apart from other cell types is their ability to undergo meiotic differentiation to from haploid gametes in gonads. The formation of mouse germ cell is accomplished by inductive interaction of the epiblast cells of early post-implantation embryo by signals emerged from the extra-embryonic tissue, which contrasts with the mode of formation of germ cells in many species by the action of germ cell determinants. Mouse primordial germ cells (PGCs) are identified conventionally by the expression of strong activity of tissue non-specific alkaline phosphatase (TNAP; encoded by *Akp2*), and *Pou5f1*, *Dppa3* and *Nanog*. However, expression of those genes are not unique to the PGCs and is found also in pluripotent cell types such as the cells of the inner cell mass (ICM), embryonic stem (ES) and embryonic germ (EG) cells.

The present study has identified five novel germ-line specific markers which were initially discovered in a subtractive screening of migratory PGCs and ICM of blastocysts (Tanaka and Matsui, Mech. Dev. 119S, S261-267, 2002). Specially, the expression pattern of two of these genes, *Lrp4* (encoding for mouse ortholog of low density lipoprotein receptor-related protein 4) and *Ipo13* (*Importin13*), has been fully characterized during mouse germ cell development. Functional analyses of *Ipo13* activity revealed a potential role of IPO13 in the nuclear-cytoplasmic trafficking of protein cargoes and the regulation of meiosis of the germ cells.

Chapter II GENERAL INTRODUCTION

Germ cells have a specialized role for transmitting genetic information to the next generation. Only germ cells have acquired the specific properties to undergo meiotic division and differentiate into haploid gametes. To understand the mechanism of germ cell formation and development will give us insights in the function of germ cells.

Germ cell formation is accomplished by the two different modes of action, the inductive interaction and the action of germ cell determinants (Wylie 1999; McLaren, 2003). In many animal species, such as *Drosophila* and *Caenorhabditis* (*C.*) *elegans*, maternal factors via the 'germ-plasm' determine the germ-line fate of embryonic cells. Blastomeres containing the germ-plasm give arise to germ cells, and others without the germ-plasm differentiated into somatic cells (Eddy 1975; Rongo and Lehmann 1996). In other species, such as in the mouse, tissue-/cell-interaction facilitates germ cell formation.

In the mouse, lineage-analysis demonstrated that germ cells are derived from the cells localized in the proximal region of epiblast of pre-streak embryo (**Fig. 1**; Lawson and Hage, 1994). Recent findings demonstrated that *Prdm1*/*Blimp1* is activated progressively in a group of cells in the proximal epiblast of the pre-gastrulating Embryonic day (E) 6.25 embryo which form primordial germ cells (PGCs) in mice (Ohinata et al., 2005). Loss of *Prdm1* function results in marked reduced number of PGCs (Ohinata et al., 2005; Vincent et al., 2005), and the few PGCs remaining display inappropriate *Hoxa1* and *Hoxb1* activity in the mutant embryo (Ohinata et al., 2005). In *Drosophila* and *C. elegans*, a period of transcriptional quiescence in the early germ cell precursors is essential the formation and survival of the germline (Leatherman and Jongens, 2003). Consistent with this, it implies

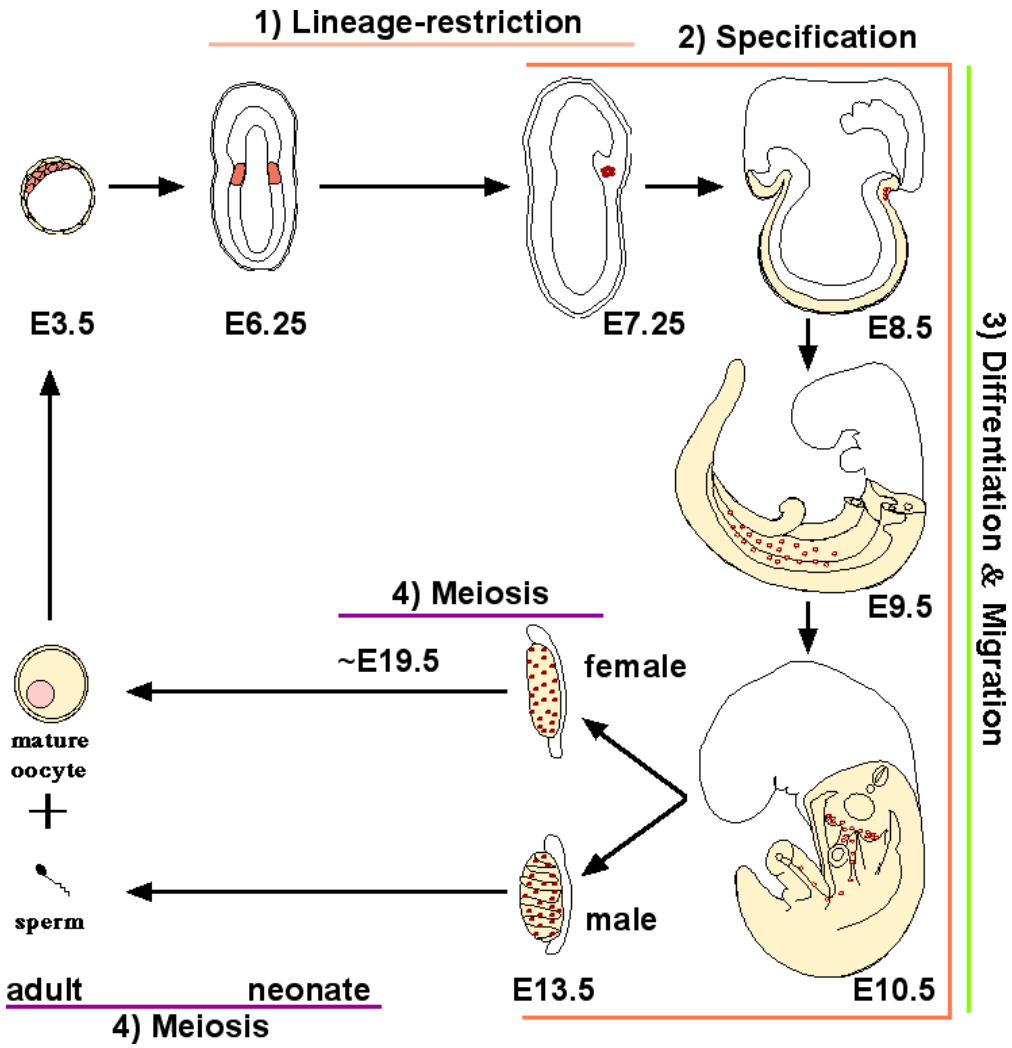

Figure 1 Four phases of mouse germ cell development; 1) lineage-restriction, 2) PGC specification, 3) PGC differentiation and migration, 4) germ cell differentiation in meiosis

Mouse germ cell precursors arise in the proximal region of epiblast of pre-streak embryo. Primordial germ cells (PGCs) are first found in the cluster at the base of allantoic bud at E7.25. Mouse PGCs are found in the endoderm derived hindgut at E8.5~9.5. After arriving at gonad region, female germ cells enter into the meiosis. On the other hand, male germ cells cease mitotic division and entry in meiosis after birth.

that the repression of somatic gene expression in germ cell precursors may facilitate mouse germ cell formation. Although *Prdm1* positive putative PGC precursors are first found in the pre-gastrulating embryo (Ohinata et al., 2005), PGCs could be derived from distal epiblast cells that did not express *Prdm1*if there were transplanted into the proximal epiblast region where they would be exposed to the inductive signals at E 6.5 (Tam and Zhou, 1996). These findings suggest that the establishment of mouse germ-line may take place progressively around gastrulation (McLaren and Lawson, 2005). Analyses on mutant mice lacking the activity of bone morphogenetic protein (BMP) signaling pathway revealed the deficient in PGC formation and/or maintenance. BMP4 and -8 activities in the extra-embryonic ectoderm (ExE) and BMP-2 activity in adjacent visceral endoderm (VE), and the BMP receptor ALK2 function in VE of the pre-gastrula embryo are required for germ cell formation (Lawson et al., 1999; Zhao and Garbers, 2002; de Sousa Lopes et al., 2004).

Mouse PGCs are first detected in E7.25 gastrula-stage embryos by the strong tissue non-specific alkaline phosphatase (AP, encoded by *Akp2*) activity in a tight cluster of the cells in the posterior primitive streak at the base of the allantoic bud (**Fig. 1**; Ginsburg et al., 1990). It was postulated that this clustering of cells might enhance the physical interaction which facilitates the specification of the PGCs (Yoshimizu et al., 2001; Saitou et al., 2002; Matsui and Okamura, 2005).

During gastrulation of the mouse embryo, PGCs transit from the mesoderm to the definitive endoderm (Anderson et al., 2000). PGCs actively proliferate and migrate from hindgut to dorsal mesentery. PGCs start to colonize the genital ridges at around E10.5 (**Fig. 1**; McLaren, 2003; Molyneaux and Wylie, 2004). In female fetal gonads, germ cells start to

enter prophase of meiotic division at E13.5 and reach the pachytene stage at around E17.5 (**Fig. 2A**; Pepling and Spradling, 2001; McLaren, 2003). By 5 days after birth, all oocytes, which are contained with a follicle composed of follicular cells, are arrested at the diplotene stage of the prophase of the first meiotic division. In the adult ovary, oocytes recommence the meiotic division and initiate follicular growth by hormonal stimuli (**Fig. 1**). On the other hands, male germ cells enter mitotic arrest at E13.5 and only recommence proliferation and differentiation in the postnatal testis (McLaren, 2003). About 10 days after birth, the meiotic germ cells differentiate into spermatogonia and resting spermatocytes (**Fig. 2B**). These primary spermatocytes reach an early pachytene stage of meiotic prophase at about 12 days after birth and it lasts for 7 days. Primary spermatocytes complete the first meiotic division and mature into secondary spermatocytes around 3-weeks after birth, and they terminally differentiate into haploid spermatids around 4-weeks after birth. Finally, they differentiate into mature sperm (**Fig. 2B**; Russel et al., 1990). During the migration, PGCs are known to express *Akp2*, *Dppa3* (*Stella*/*PGC7*), and *Pou5f1* (*Oct-3*/*4*) (MacGregor et al., 1995; Saijoh et al., 1996; Pesce et al., 1998; Sato et al., 2002; Saitou, et al., 2002; Payer et al., 2003). However, these molecular markers are also expressed in cell types other than the germ cells including the embryonic stem (ES) and embryonic germ (EG) cells. Functional analyses of these genes did not show the essential role in PGC formation and development. For example, *Akp2* mutant mice (MacGregor et al., 1995) and *Dppa3* null offspring (Payer et al., 2003) did not show any abnormality in germ cell development. However, *Dppa3* null female mice displayed reduced fertility due to a lack of maternally inherited DPPA3 protein in their oocytes (Payer et al., 2003). *Pou5f1* and *Nanog* show crucial roles in the embryonic

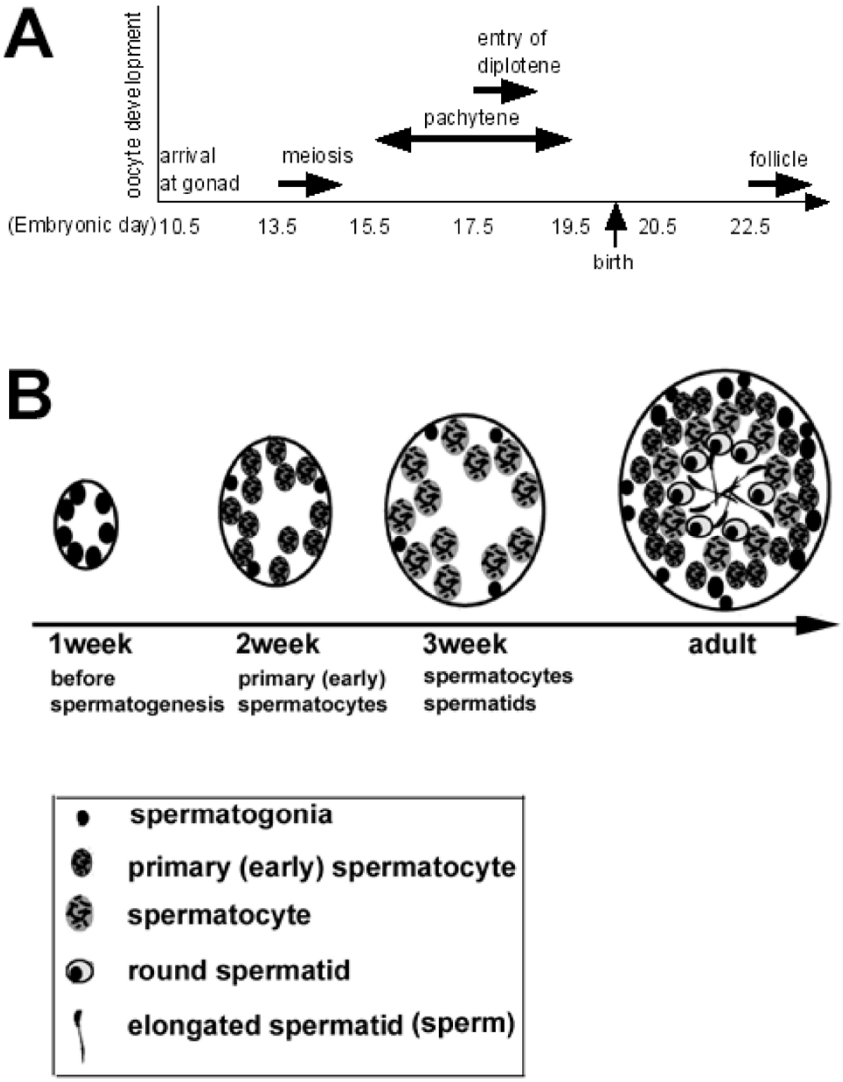

Figure 2 Mouse germ cell differentiation in meiosis
Female germ cells enter into the meiosis at E13.5 and reach the pachytene stage at around E17.5 (A). Male germ cells cease mitotic division and entry in meiosis after birth in seminiferous tubule, reach an early pachytene stage of meiotic prophase at around 2-weeks and mature into secondary spermatocytes around 3-weeks (B).

lineage specification in the blastocyst or epiblast of the early implanted embryo development, but their functions in germ cells remain unclear (Nichols et al., 1998; Chambers et al., 2003; Mitsui et al., 2003).

To identify specific markers that may distinguish germ cells from the stem cells in early embryos, a subtractive screening of cDNAs isolated from migratory PGCs of E8.5-9.5 embryos and the inner cell mass (ICM) of E3.5 blastocysts was performed (Tanaka and Matsui, 2002). Five genes that are differentially expressed in the PGCs were isolated (**Fig. 3**). Two out of them are mouse orthologs of interferon-induced transmembrane protein (*Ifitm*) genes 1 (*mil-2)* and –3 (*mil-1/fragilis*) (Tanaka and Matsui, 2002).

Ifitm3 was also identified independently in a screen of transcripts expressed in single presumptive PGCs of the mouse gastrula (*fragilis*; Saitou et al., 2002). During germ cell formation, *Ifitm1* expression is detected in precursors of PGC and is down-regulated in PGCs. *Ifitm1* is re-expressed in the migratory PGCs homing to the urogenital ridges and in gonadal germ cells. *Ifitm3* expression is detected in precursors of PGC at an earlier stage than *Ifitm1* expression, and is continuously expressed in migratory and gonadal PGCs (Saitou et al., 2002; Tanaka and Matsui, 2002; Lange et al., 2003; Tanaka et al., 2004). During the relocation of PGCs from the mesoderm to the embryonic definitive endoderm, *Ifitm1* expression is found in the mesoderm but not in PGCs, and *Ifitm1* activity is required for the repulsive guidance of PGC transition from the mesoderm to the endoderm. In contrast, *Ifitm3* expression in PGCs may play a role in the homing guidance of PGCs regionalizing to posterior hindgut endoderm (Tanaka et al., 2005).

This project focuses on the characterization of the other two candidate genes, *Ipo13*

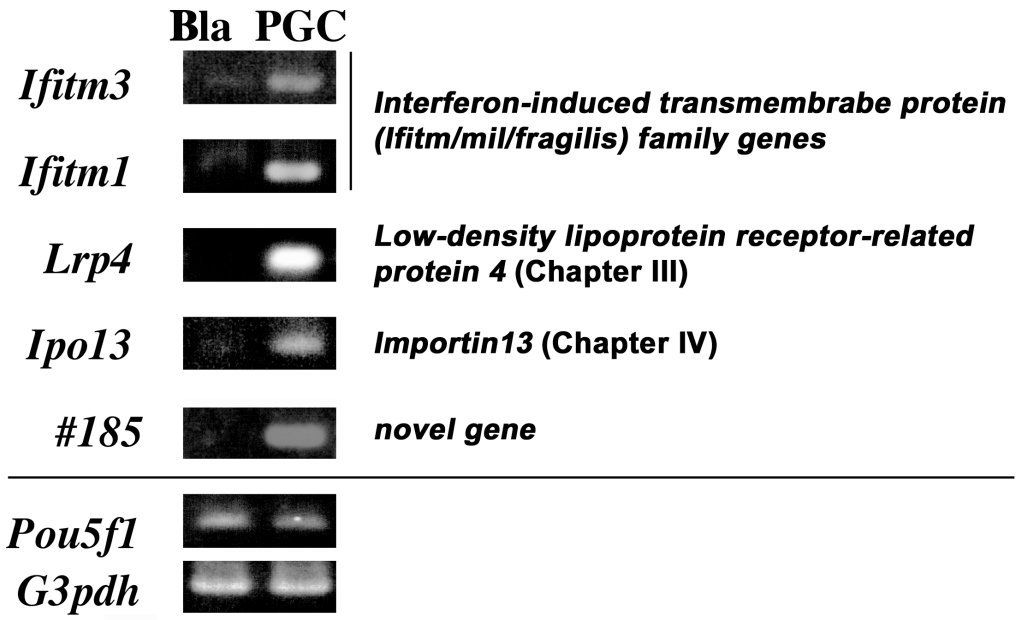

Figure 3 Candidate genes identified by a subtractive screening of migratory primordial germ cells and the blastocyst
Five cDNAs are differentially expressed in the primordial germ cells (PGCs) (Tanaka and Matsui, 2002). *Ifitm1* activity is required for PGC repulsion from mesoderm to endoderm; in contrast, *Ifitm3* expression may play a role in PGC homing to posterior hindgut endoderm (Tanaka et al., 2005). *Lrp4* is expressed in migratory and gonadal germ cells (Chapter III). *Ipo13* plays a role in stage-specific nuclear-cytoplasmic translocation of cargo which may regulate the meiotic differentiation of the mouse germ cells (Chapter VI). #185 is a novel gene, which shows stage-specific expression in meiotic germ cells (unpublished data). Bla, blastocyst. PGC, collected PGCs from E8.5~9.5 embryos. As controls, expression of *Pou5f1*, a marker of primordial germ cells and *G3pdh* were included in the assays.

and *Lrp4* (Chapter III and IV-i). Further analysis was performed on the functional role of IPO13 in a regulation of meiotic differentiation of the germ cells (Chapter IV-ii and -iii).

Chapter III Expression pattern of mouse ortholog of *LRP4* in mouse germ cells

1. INTRODUCTION

Members of low density lipoprotein receptor-related protein (LRP) family are involved in the cellular uptake of extra-cellular ligands and regulate diverse biological process in including lipid and vitamin metabolism and cell-surface protease activity, and play a role of multi-functional receptors in nervous system (Herz and Bock, 2002).

Human LRP4/MEGF7, which encodes a LDL receptor like protein with multiple EGF-like motifs, was originally identified by bio-informatic analysis of human brain cDNA clones that contain EGF-like motif (Nakayama et al., 1998). Mouse *Lrp4*/*Megf7* gene, which encodes a 7.8kb full size transcript, was previously known as *LDLR dan* in the NCBI database (Simon-Chazottes et al., 2000). LRP4 is reputed to be an integral component of the cell membrane and is predicted to function in calcium binding, receptor activity and endocytosis (FANTOM consortium, 2002; Nykjaer and Willnow, 2002). The structural organization of the extra-cellular domain especially four of EGF-like motifs of LRP4 closely resembles that of another LRP family, LRP5 and LRP6, which are known to act as co-receptor of Wnts (**Fig. 4C**, Pinson et al., 2000; Herz and Bock, 2002).

Lrp6 mutant embryos exhibit axial truncation due to reduction in the size of the tail bud, neural tube closure defects, and abnormal patterning of the limb bud, the phenotype is reminiscent of that associated with loss of Wnt function (Pinson et al., 2000). The related family member, *Lrp5* is widely expressed in embryo (Hey et al., 1998) and may limit the *Wnt*-phenotypes observed in *Lrp6* mice (Pinson et al., 2000). Another member of *Lrp* family

genes, *Lrp1*, which gene activity plays a role in the action of receptor of variously lipo-proteins, is abundantly expressed in hepatocytes and neurons. *Lrp1* knockout mice die during early and mid-gestation due to the deficient in implantation (Herz et al., 1992; Herz and Bock, 2002). Therefore, the expression patterns of *Lrp* family genes including *Lrp4* in germ cells have not been reported.

In this chapter, the analysis of the expression of *Lrp4* reveals that this gene is expressed in migratory PGCs and matured germ cells, but not in the blastocyst, the epiblast, and the ES and EG cells.

2. RESULTS

The subtractive screening of cDNA of migratory PGCs and the blasotcysts identified a 300bp partial sequence of the 3'-UTR of *Lrp4* (f1, **Fig. 4B**; accession number; NM_172668) (**Fig. 4A**). The predicted amino acid sequences of mouse LRP4 (1905 amino acids) were similar to that of human (95.0%) and rat (98.1%) protein (**Fig. 5**). The structural organization of LRP4 and another LRP family, LRP5/6 and LRP1, are shown in **Fig. 4C**.

The predicted protein structure of the extracellular domain of LRP4 closely resembles to one of LRP5/6 (**Fig. 4C**). On the other hand, the intracellular domain of LRP4 has a copy of NPXY motif, and LRP1 also has NPXY motifs, but LRP5/6 has no NPXY motif (**Fig. 4C**; Herz and Bock, 2002; Johnson et al., 2005).

The differential expression of *Lrp4* was validated by RT-PCR analysis of total RNA pools of the blastocysts, the tissue of the dorsal mesentery of E9.5 embryo and the E13.5 gonads pooled from both sexes (**Fig. 6A**). Consistent with the result of the cDNA subtractive screening, *Lrp4* was expressed in the tissues of the dorsal mesentery and the gonads that contain PGCs, but not in the blastocyst (**Fig. 6A**). *Lrp4* was also not expressed in the embryonic stem (ES) cells, the embryonic germ (EG) cells or the STO feeder cells (**Fig. 6B**). The absence of *Lrp4* expression in the ES cells implicates that *Lrp4* is not expressed in the *Pou5f1*-expressing ICM cells from which the ES cells are derived. In the adult mice, *Lrp4* was expressed in the testis and ovary, and also in the kidney and brain (**Fig. 6C**).

Whole mount *in situ* hybridization revealed that *Lrp4* expression was not detectable in the E6.5 early-gastrula embryo (**Fig. 7A**) and was weakly expressed in the allantoic bud and the amnion of the E7.5 late-bud stage embryo (**Fig. 7B, B'**). In the E9.0 embryo, strong

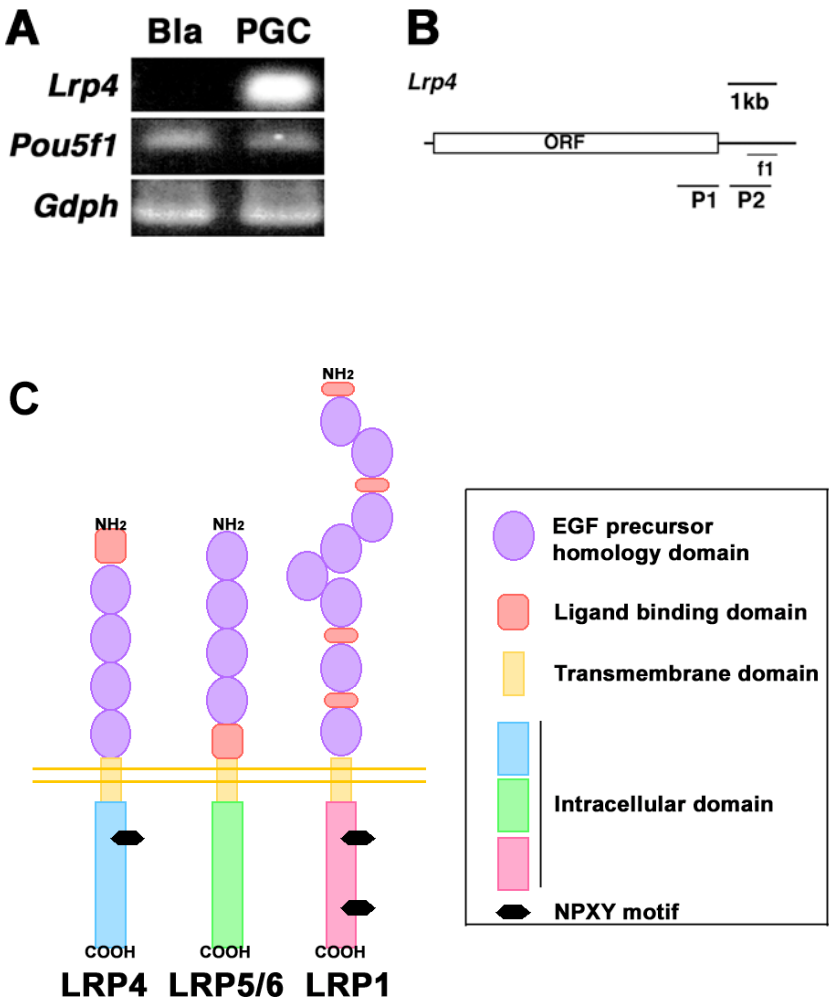

Figure 4 Cloning of mouse ortholog of *Lrp4*.
PCR amplification of *Lrp4* from cDNA prepared from blastocysts (Bla) and the Pou5f1-GFP expressing primordial germ cells (PGC) of E9.5 embryo (A). *Lrp4* mRNA containing the putative open reading frame (ORF), identified by the f1 fragment in the PGC cDNA library (B). Comparison of structure between LRP4, LRP5/6 and LRP1 (C). P1: riboprobe for *in situ* hybridization, P2: probe for Northern analysis.

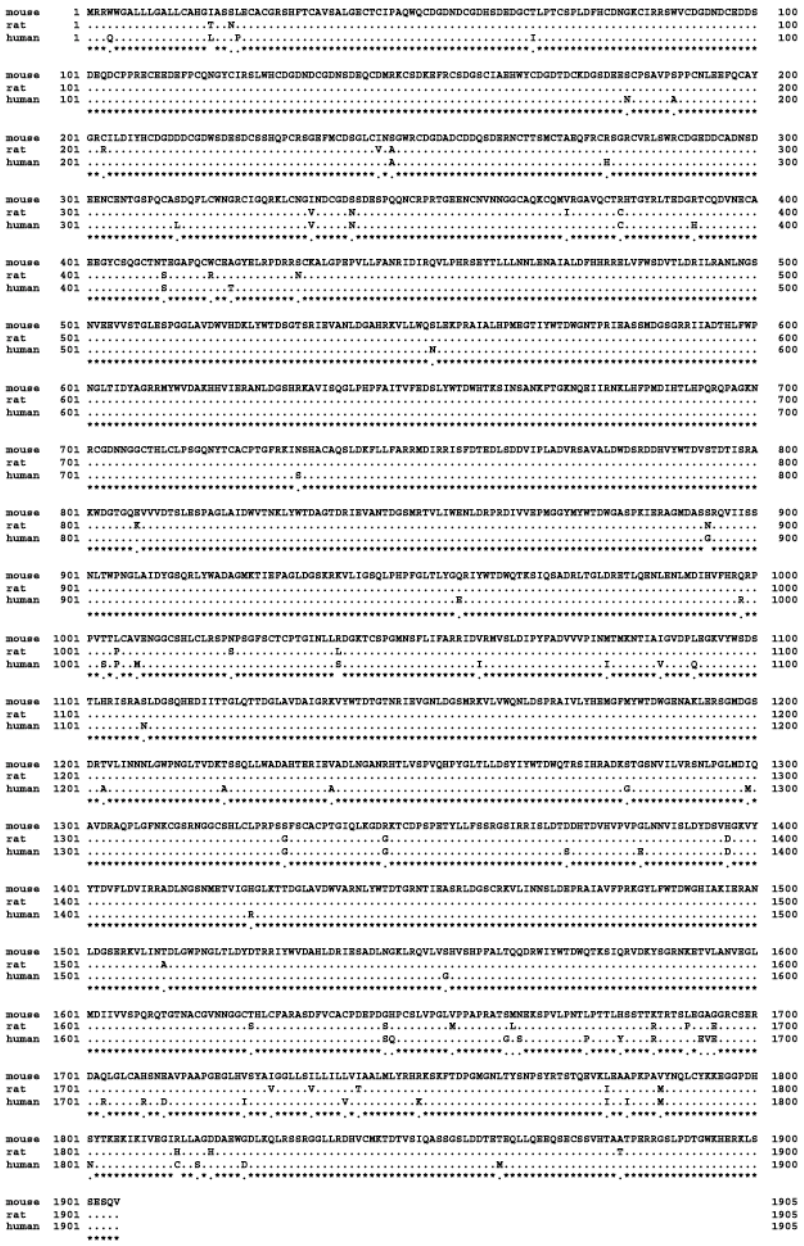

Figure 5 Alignment of LRP4 proteins

Comparison of putative amino acid sequences of LRP4 protein (1905 amino acids) of mouse, rat and human. The predicted mouse LRP4 amino acid sequences were similar to that of human (95.0%) and rat (98.1%) protein.

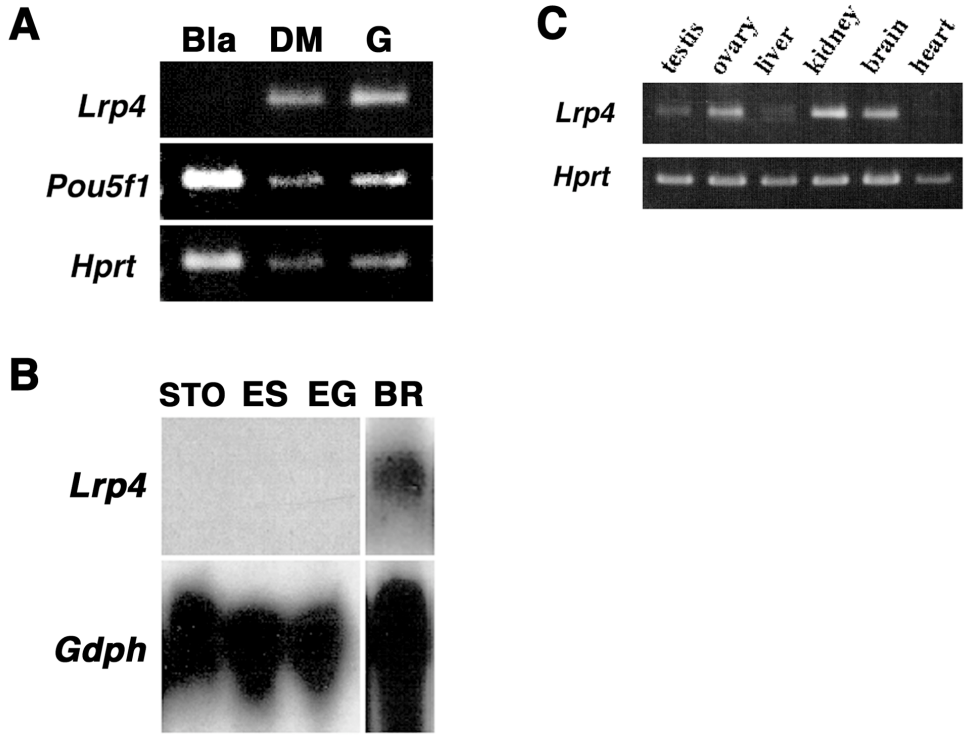

Figure 6 Expression profile of *Lrp4* in embryonic and adult tissues and cell lines
(A) *Lrp4* expression is absent from the *Pou5f1*-positive blastocyst (Bla) but is co-expressed with *Pou5f1* in the tissue of the dorsal mesentery (DM) and the gonads (G) of E13.5 embryos (samples pooled for both sexes), analysed by RT-PCR. (B) No expression of *Lrp4* in STO feeder cells, D3 ES cell and EG (EG1) cells was detected by Northern analysis. *Lrp4* expression in the adult brain tissue (BR) was shown as a control. (C) Expression of *Lrp4* in adult testis, ovary, liver, kidney, brain and heart by RT-PCR analysis. Expression of *Hprt* and *Gdph* provided the loading controls.

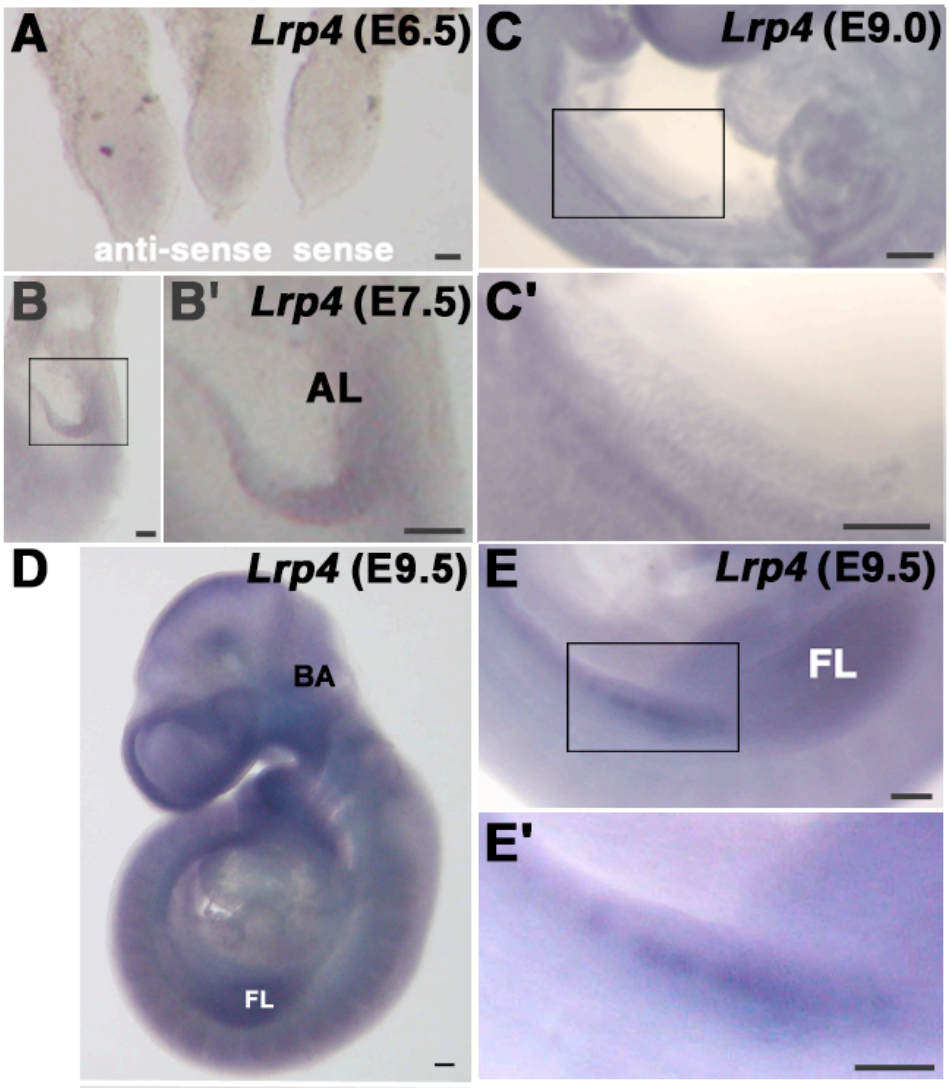

Figure 7 ***Lrp4*** **expression in postimplantation embryos.**
Undetectable expression in the early-streak (E6.5) embryo (A). Weak expression in allantoic bud and the amnion of the E7.5 late-bud stage embryo (B and B', B': an enlarged view of the boxed region in B; AL, allantoic bud; posterior to the right). Expression was not detected in E9.0 hindgut (C and C', C': an enlarged view of the boxed region in C). Whole embryo at E9.5 (D). BA, branchial arches. Expression in the forelimb bud and the urogenital ridges of the E9.5 embryo (E and E', E': an enlarged view of the boxed region in E; FL, forelimb). Bars =40μm.

Lrp4 expression was not detected in any tissue including hindgut where PGCs are localized (**Fig. 7C, C'**) but was present in the cells in the urogenital ridges of E9.5 embryo (**Fig. 7E'**). *Lrp4* was also expressed in the branchial arches (**Fig. 7D**), and the forelimb bud of the E9.5 embryo (**Fig. 7D, E**).

The co-expression of *Lrp4* and *Pou5f1* in the dorsal mesentery and the fetal gonad (**Fig. 6A**) suggests that *Lrp4* may be expressed in the germ cells. To determine if *Lrp4* is expressed specifically in the germ cells, double *in situ* hybridization was performed to detect the co-expression of *Lrp4* and *Pou5f1*. In the E9.5 embryo, weak *Lrp4* expression was detected in the *Pou5f1*-expressing PGCs in the dorsal region of the hindgut (**Fig. 8A, B-B"**). A strong *Lrp4* expression was detected in the *Pou5f1*-expressing PGCs in the dorsal mesentery (**Fig. 8C, D-D"**), the *Pou5f1*-positive germ cells in the genital ridge of E10.5 (**Fig. 8E, F-F"**) and E11.5 embryos (**Fig. 8G, H-H"**), and the *Pou5f1*-positive germ cells in the fetal testis (**Fig. 8I, J-J"**) and fetal ovary (**Fig.8K, L-L"**) of E13.5 embryos. *Lrp4* expression is therefore specific to the germ cells during the migration from the hindgut to the fetal gonad.

In the E16.5 fetal testis, *Lrp4* was expressed in the DDX4/MVH-positive germ cells in seminiferous tubules (**Fig. 9A, B**; Toyooka et al., 2000). In the neonatal testis, the spermatogonia that are localized to the central region of the seminiferous tubules and positive for TRA98 immunoreactivity (**Fig. 9C**; Tanaka et al., 1997) expressed *Lrp4* (**Fig. 9D-D'**). Similarly in the adult testis, *Lrp4* was also strongly expressed in the TRA98-positive spermatogonia (**Fig. 9E, F-F'**). However, *Lrp4* expression was restricted mainly to the spermatogonia and was not detected in mature spermatocytes or haploid spermatids (**Fig. 9**

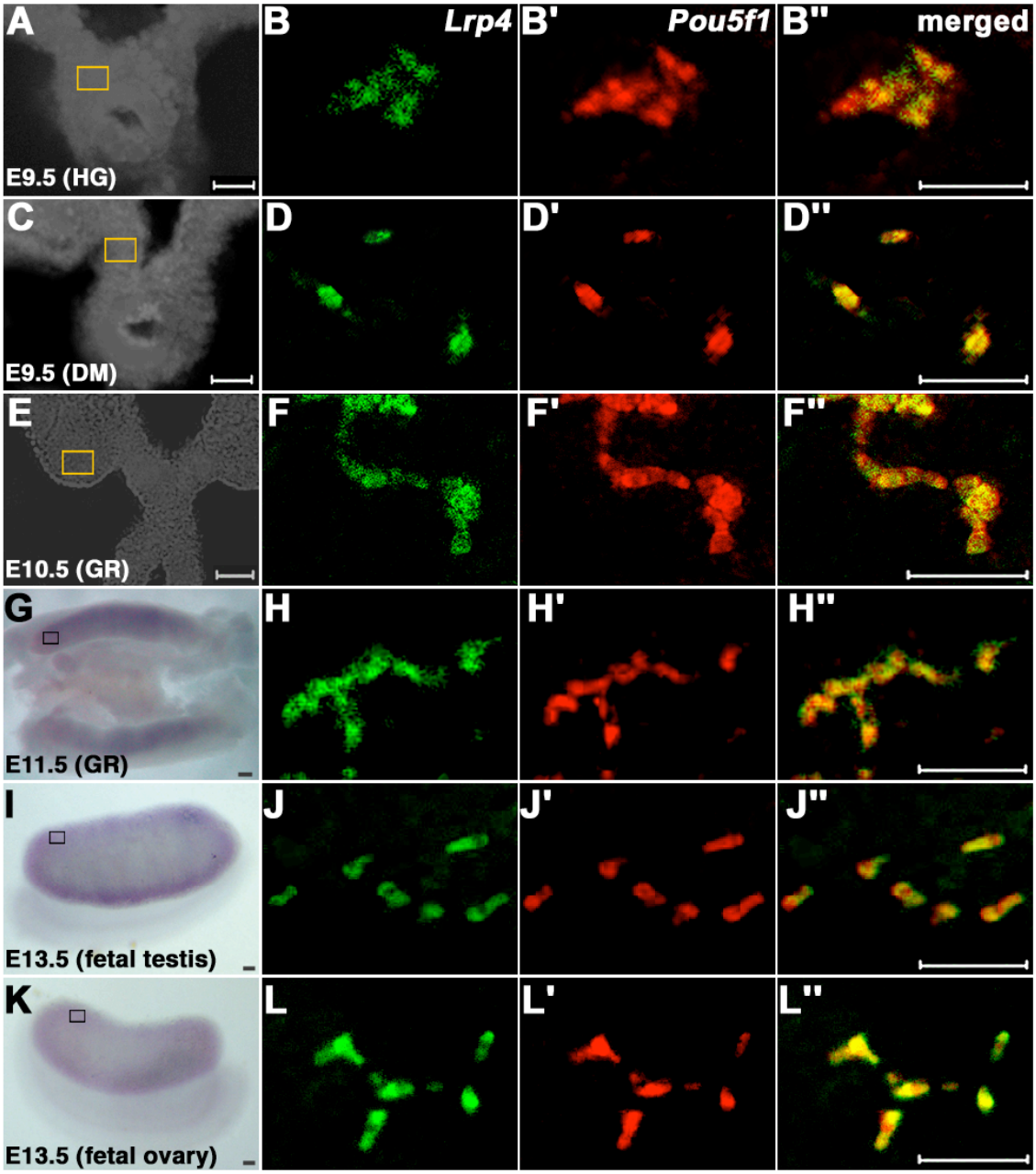

Figure 8 Expression of *Lrp4* in *Pou5f1*-expressing PGCs by double *in situ* hybridization

(A, B-B") the hindgut (HG) and (C, D-D") the dorsal mesentery (DM) of E9.5 embryo, (E, F-F") the genital ridge (GR) of E10.5 embryo and (G, H-H") E11.5 embryo, and (I, J-J") the fetal testis and (K, L-L") the fetal ovary of E13.5 embryos. (A, C and E) Bright field images of the tissue (yellow box marks the region shown in higher resolution confocal image). (G, J and K) Whole mount genital ridges showing *in situ* hybridization for *Lrp4* expression (black box marks the region shown in higher resolution confocal image). (B'', D'', F'', H'', J'', L") Merged images showing co-expression of *Lrp4* (B, D, F, H, J, L) and *Pou5f1* (B', D', F', H', J', L') in the germ cells. Bars =40μm.

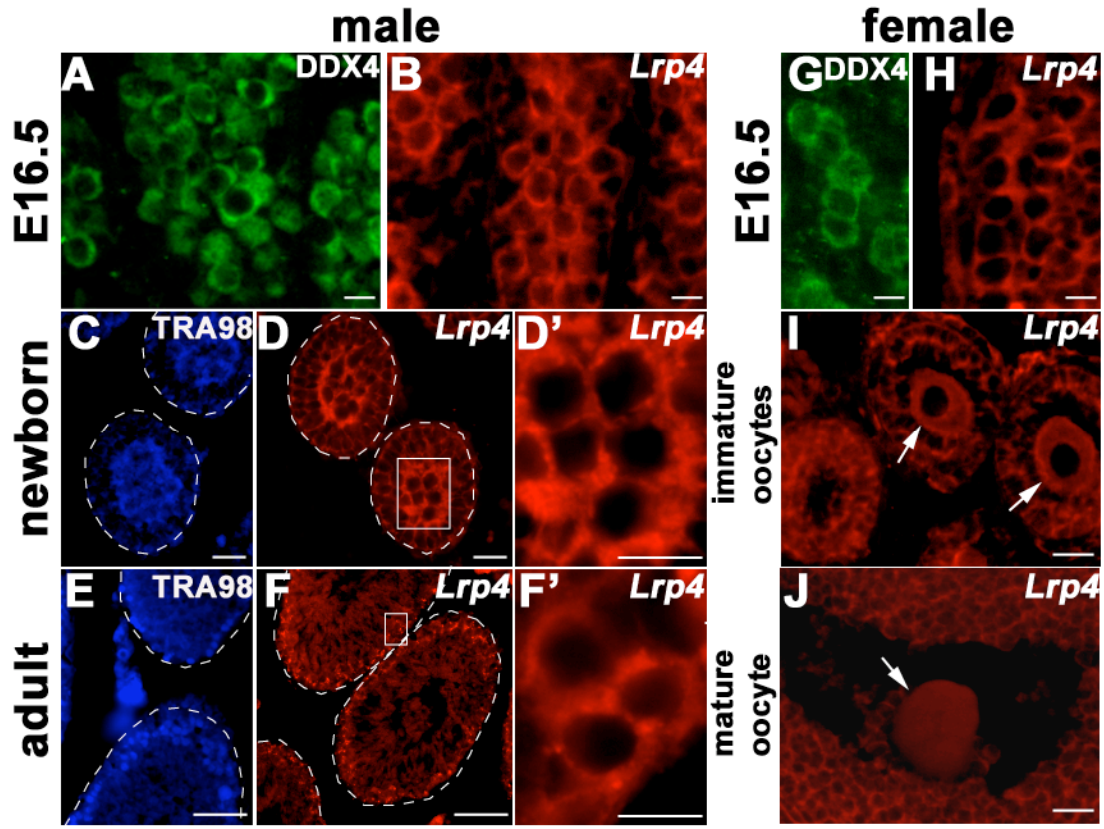

Figure 9 ***Lrp4*** **expression in developing and adult gonads.**
(A) DDX4/MVH-positive germ cells in the seminiferous tubules of the E16.5 fetal testis. (B) *Lrp4* expression in germ cells in the seminiferous tubules of the E16.5 fetal testis. Immunoreactivitiy of TRA98 was found in spermatogonia in the newborn (C) and adult (E) testis. (D) *Lrp4* expression in the spermatogonia in the newborn testis (D': an enlarged view of the boxed region) and (F) the adult testis (F': an enlarged view of the boxed region) White-doted lines outline the seminiferous tubules (C, D, E, F). (G) DDX4 positive germ cells in E16.5 fetal ovary expressed (H) *Lrp4*. In the adult ovary, *Lrp4* was expressed in immature oocytes (arrows), as well as in follicular cells (I), but only weakly in mature oocyte (J, arrow). Bars =10 μm (A-D', F', G, H). Bars=40 μm (E, F, I, J).

F). In the E16.5 female gonads, *Lrp4* was expressed in the DDX4-positive meiotic germ cells (**Fig. 9G, H**). In the adult ovary, *Lrp4* expression was found in the immature oocytes (**Fig. 9I**, arrows), and in follicular cells (**Fig. 9I**). *Lrp4* expression was down-regulated in the maturing oocytes (**Fig. 9J**, arrow).

3. DISCUSSION

In the mouse, *Akp2*, *Pou5f1*, *Dppa3* and *Nanog* are expressed in the migratory PGCs and also detected in the ICM of blastocysts, ES cells, the ICM-derived epiblast in the early post-implantation embryos and the EG cells (MacGregor et al., 1995; Saijoh et al., 1996; Pesce et al., 1998; Sato et al., 2002; Saitou, et al., 2002; Chambers et al., 2003; Mitsui et al., 2003; Payer et al., 2003; Yamaguchi et al., 2005). The present results showed that *Lrp4* expression is specific to the migratory PGCs and the germ cells in the gonad, and is not detectable in the blastocyst, the epiblast, and the ES and EG cells. *Lrp4* expression therefore provides a molecular signature that distinguishes the germ-line cells from the other pluripotent cell types in the early mouse embryo.

The structural organization of the extra-cellular domain of LRP4 closely resembles that of LRP5 and LRP6, co-receptors of Wnts, while the inter-cellular domain of LRP4 is different from one of LRP5/6. Consistent with this structure difference, co-expression of *Lrp4* with *Lrp5/6* showed the inhibition of Wnt-signaling in the transfected cells *in vitro* (Johnson et al., 2005). In addition, co-expression of LRP1 with LRP5/6 also showed the inhibition of Wnt signaling, and both *Lrp1* and *Lrp4* have NPXY motif in their intercellular domains, but the function of NPXY motif in the signal transduction of Wnts is still unknown (Johnson et al., 2005).

The function of *Megf7/Lrp4* has recently been studied by loss-of-function mutation of *Lrp4* in the mouse (Johnson et al., 2005). The knock-out mice were growth-retarded, with fully penetrant polysyndactyly in their fore and hind limbs (Johnson et al., 2005). Developmental abnormality was apparent in E9.5 limb bud, when *Lrp4* is expressed in the

apical ectodermal ridge (AER). The abnormal limbs show thickening of the AER (Johnson et al., 2005). Ectopic expression of several molecular regulates of limb patterning, including *Fgf8*, *Shh*, *Bmp2*, *Bmp4* and *Wnt7a*, and WNT- and BMP-responsive transcription factors *Lmx1b* and *Msx1*, accompanies reduced apoptosis and expansions of the AER (Johnson et al., 2005).

Lrp4 expression is found in PGCs. *Lrp4*, however, is not expressed in ICM, ES cells, and EG cells implying that *Lrp4* expression in PGCs will be down-regulated during EG cell formation. Recently, Sato et al. (2004) reported that Wnt-signaling is required the self-renewal of pluripotent ES cells. Activation of Wnt-signaling by glycogen synthase kinase (GSK)-3-specific inhibitor maintains self-renewal and the expression of pluripotent state-specific transcription factors in ES cells (Sato et al., 2004). From these results, it implies that a loss-of *Lrp4* activity may lead to loss of tissue potency in the limb bud cells, which may under in abnormal limb development. During PGC differentiation, *Lrp4* expression is up-regulated in migratory PGCs before onset of homing to embryonic gonads (**Fig. 6E, E', Fig. 7A-F''**), and Wnt ligands are known to be expressed in the region near the genital ridge. For example, *Wnt-4* expresses in the genital ridge and this gene activity is required for the embryonic female gonad development (Vainio et al., 1999). In the *Wnt-4* mutant embryo, a postmeiotic loss of oocytes was also found, but it is still unclear that WNT-4 signaling appears to be directly or indirectly involved in differentiation of the female germ line. It is predicted that *Lrp4* is required for the inhibition of the activation of Wnt-signaling in PGCs, which may be involved in PGCs proliferation and/or differentiation. Consistent with this concept, a lack of the tumor suppressor gene, *Pten*, which is involved in the suppression of Wnt-signaling

pathway in germ cells, leads to enhance the efficiency of EG cell formation from germ cells in the embryonic gonad (Kimura et al., 2003). Their recent literature also reported that a stabilization of β-catenin, which is a signal-transducer of canonical Wnt signaling, is involved in cell cycle progression in PGCs (Kimura et al., *in press*). However, germ cell development in the *Lrp4* mutant mouse embryo was not investigated. Further analysis of *Lrp4* activity in germ cells will give us a new insight in the molecular mechanism of germ cell differentiation and EG cell formation.

Chapter IV Stage specific expression of *Importin13* is required in meiotic germ cell differentiation

1. INTRODUCTION

Ipo13 gene is a one of the *Importinβ* family, which encodes nuclear and cytoplasmic transport factors, and mammal cell has about 22 putative members. Members of this family are accountable for the recognition of the majority of nuclear transport cargo, and through the nuclear pore complex to shuttle between nuclear and cytoplasm depending on Ran-GTPase gradient rule (Strom and Weis, 2001; Weis, 2003). Nucleo-cytoplasmic trafficking of cargo molecules by Importins is crucial for cell functions, such as the cell cycle progression and proliferation, the transduction of signaling activities and the regulation of cell differentiation (Yoneda, 2000; Weis, 2002). However, regulatory mechanisms of the stage-specific translocation of cargo molecules are still unclear.

In *Drosophila*, several *Importins* are expressed in successive stages of spermatogenesis (Giarre et al., 2002): *Importin-α2* is expressed in the spermatogenic cell spanning the spermatogonial stage to the end of second meiotic division. *Importin-α1* is expressed in the germ cells till they differentiate into early spermatids and *Importin-α3* is expressed in post-meiotic cysts. Loss of function of *Importin-α2* blocks spermatogenesis, and leads to the production of defective sperm and male sterility (Giarre et al., 2002; Gorjanacz et al., 2002; Mason et al., 2002). The sterility could be rescued by reconstituting *Importin-α2* activity or by expressing *Importin-α1* or *-α3* (Mason et al., 2002), pointing to a functional overlap of these three *Importins*. In *C. elegans, Importin-α1*, *–α2* and *–α3* are expressed in germ line cells (Geles and Adam 2001). Specifically, RNAi experiments

demonstrate that Importin-α3 protein is required for the progression of meiotic prophase I during oocyte development (Geles and Adam 2001). However, the expression of these *Importins* is not specific to the stage when these mutants show the defects in germ cells, and the cargoes of these *Importins* are also unknown. In the mouse testis, orthologs of *Importin-β* (*Importin-β1*/*Kpnb1*) and *Importin5* (*Importin-β3*/*Ranbp5*/*Kpnb3*) are expressed in the spermatogenic cells (Anway et al., 2003; Loveland et al., 2005) in addition to *Ipo13*, which is identified in the present study. However, the functional roles and cargoes of Importin-*β* and *Importin5* in the meiotic germ cells are still not known.

Mingot et al. identified human *Ipo13* gene by the bioinformatic analysis of human expression sequence tags (ESTs), and they demonstrated that human IPO13 works for both of an importer and exporter of the specific cargo (Mingot et al., 2001). Human IPO13 mediates specific nuclear import of ubiquitin-conjugating enzyme 9 (UBC9), RNA-binding motif protein 8 (RBM8), and human homologue of *Drosophila* mago nashi protein (MGN), and it also mediates nuclear export of eukaryotic translation initiation factor 1A protein (Eif1a) protein (Mingot et al., 2001). Human IPO13 interacts with UBC9, and specifically mediates nuclear localization of UBC9 in HeLa cells solely, but not by another Importins (Mingot et al., 2001). Rat *Ipo13* gene also identified by the representational difference analysis to search for glucocorticoid-inducible genes in developing lung of fetal rat, and it also referred to *late gestational lung 2* (*LGL2*) gene (Zhang et al., 2000). Rat *Ipo13* is differentially expressed in fetal lung (maximal during the pseudoglandular stage, gestational Days 14 to 16), induced by glucocorticoid, and enriched in epithelium relative to the mesenchyme during fetal lung organogenesis (Zhang et al., 2000).

Here, I investigated the stage-specific expression of *Ipo13* in meiotic germ cells and the potential role of *Ipo13* activity in meiotic differentiation.

2. RESULTS

2-i. Stage specific expression of *Importin13* in germ cells

A cDNA clone *#B94*, which encoded a 308bp partial sequences of mouse *Importin13* gene (*Ipo13*, accession number; NM_146152, **Fig.10**) was identified by subtractive screening of the cDNA of migratory PGCs (E8.5-9.5) and E3.5 blastocysts (**Fig. 11A**; Tanaka and Matsui, 2002).

By RT-PCR analysis, *Ipo13* transcript is detected in the hindgut and fetal gonads but not in blastocysts (**Fig. 11B**). Northern blot analysis using the *#B94* fragment as a probe showed expression of 3.4kb *Ipo13* transcript predominantly in the adult testis, brain and kidney (**Fig. 11C**). In the adult testis, a 1.6kb transcript, which was not reported previously, is also expressed (**Fig. 11C**).

These two different size cDNAs were identified 5' and 3' rapid amplification of cDNA ends (RACE) of #B94 fragment in adult testis using Marathon cDNA amplification kit (Clontech). 5' RACE leads to show two partial cDNA products and 3' RACE also does one cDNA product of the putative full-length aDNA of #B94. By the sequencing, these RACE products are matched to mouse *Ipo13*. By the end-to-end PCR analysis and sequencing, two transcripts were obtained from the RACE products: first one encoded a full-length of mouse orthologue of *Ipo13* gene, and another short one also encoded mouse *Ipo13* gene but its transcriptional start site was found in 6th intron of mouse *Ipo13* genome (**Fig. 10**). These results are consistent with the result of Northern blot and suggest that two transcripts of mouse *Ipo13* are arose as a result of the utilization of different transcription start sites. These two transcripts are therefore designates as long form of full-length mouse *Importin13*

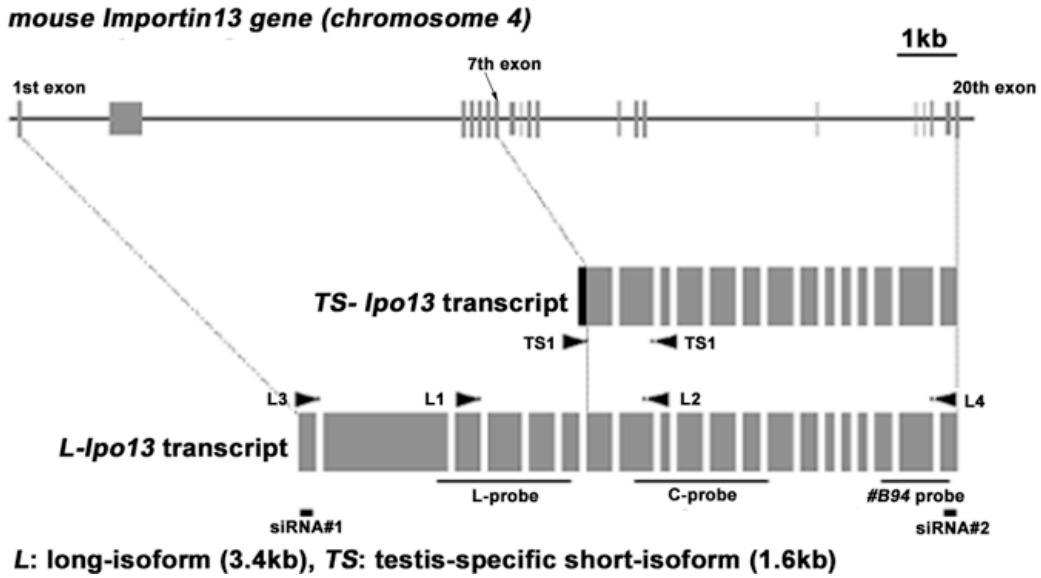

Figure 10 Genomic structure of *Ipo13*

The mouse *Ipo13* gene encodes two transcripts via the utilization of different transcription start sites. The full-length transcript (*L-Ipo13*) contains the coding sequences of all 20 axons. The shorter testis-specific (*TS-Ipo13*) transcript contains 75 bp sequence (black box) of 6th intron and the sequence of the 7th to 20th axons of the gene. The genomic regions corresponding to *#B94* partial cDNA fragment, the L-probe (that is specific for the full-length transcript), the C-probe (which detects both the full length and the short transcript) are underlined. The sequences targeted by the siRNA reagents: siRNA#1 and siRNA#2 are indicated by the bold bars, and those recognized by L1, L2, L3, L4, TS1 and TS2 primers are indicated by arrowheads.

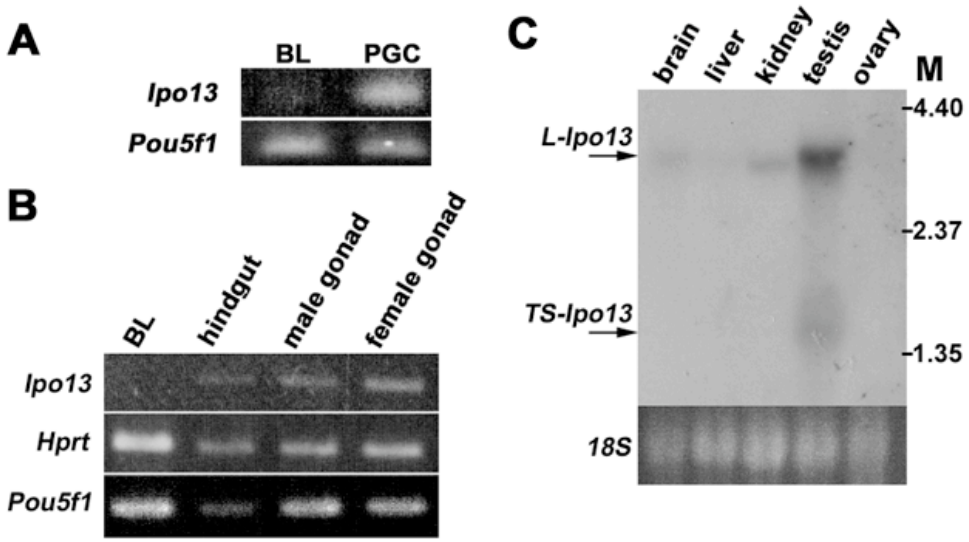

Figure 11 ***Ipo13*** **expression in fetal and adult tissues**
A: PCR amplification of *Ipo13* from cDNA prepared from blastocysts (BL) and the *Pou5f1-GFP* expressing primordial germ cells (PGC) of E8.5-9.5 embryos.
B: Expression of *Ipo13* in hindgut and fetal gonads of both sexes which contain *Pou5f1*-expressing germ cells. *Ipo13* is not expressed in the *Pou5f1*-expressing inner cell mass of the blastocyst (BL). *Hprt*, loading control.
C: Expression of *L-Ipo13* and *TS-Ipo13* in the adult tissues by Northern blot analysis. M, molecular size; *18S*, loading control.

(*L-Ipo13*) and testis-specific short *Importin13* (*TS-Ipo13*). *TS-Ipo13* cDNA has 75bp of 6th intron sequences and from 7th to 20th exons of *L-Ipo13* gene (**Fig. 10**). Moreover, the putative protein (963 amino acids, L-IPO13) encoded by the *L-Ipo13* transcript is conserved between mouse, human (99.2%) and rat (98.8%), and the putative 438 amino acids protein (TS-IPO13) encoded by the *TS-Ipo13* transcript is identical to the C-terminal fragment of L-IPO13 (**Fig. 12A**). Western blot analysis with anti-IPO13 antibody in the adult testis revealed two bands for full-length L-IPO13 and predicted TS-IPO13, respectively (**Fig. 12B**).

The expression of *L-Ipo13* in PGCs was confirmed by double probed whole mount *in situ* hybridization of E9.5 embryos and E13.5 gonads using ribo-probes for *Pou5f1* and *L-Ipo13* genes respectively (**Fig. 13)**. In E9.5 embryos, *L-Ipo13* is expressed in the *Pou5f1* positive PGCs in the hindgut (**Fig. 13A-A''**). *L-Ipo13* and *Pou5f1* are also co-expressed in the germ cells of the male (**Fig. 13B-B"**) and female E13.5 gonad (**Fig. 13C-C''**).

To further elucidate the expression profiles of *Ipo13* genes in germ cells, I examined the expression of *L-Ipo13* and *TS-Ipo13* in developing fetal and adult gonads. *L-Ipo13* transcript is expressed in the gonad of the fetus, the neonatal (1-week-old) and adult mice of both sexes (**Fig. 14A**). A significantly stronger signal was detected in the E17.5 fetal ovary and the adult testis in which a substantial population of meiotic germ cells is present. In contrast, *TS-Ipo13* is detected only in the adult testis (**Fig. 14A**).

In the male gonads, the expression profile of *L-Ipo13* and *TS-Ipo13* was examined in a finer time scale in the testes of 1-, 2-, 3-week-old and adult (more than 6-weeks) mice to determine the stage when the strong *Ipo13* expression commences. *L-Ipo13* expression reaches the adult level at 3-weeks-old testis, when many spermatocytes have reached the

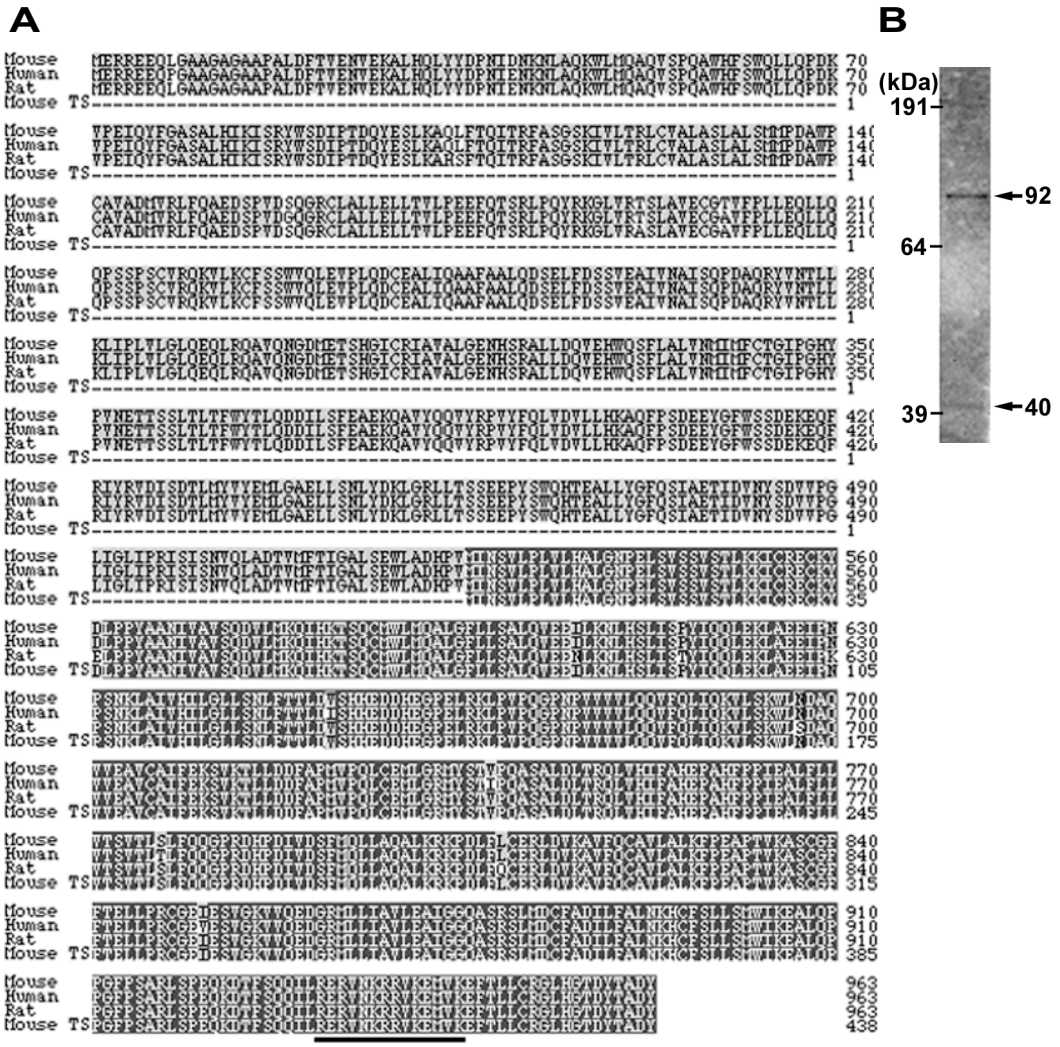

Figure 12 (A) Comparison of putative amino acid sequences of *Ipo13* of the full length (IPO13: 963 amino acids) and the testis-specific (TS-IPO13: 438 amino acids) proteins, and that of the rat and human. TS-IPO13 is identical to the C-terminal part of IPO13. Under line is showing position of antigen sequence of anti-Ipo13 antibody. (B) Western blot analysis with the anti-Ipo13 antibody in the adult testis revealed two different sizes of protein: full-length L-IPO13 (Ca. 92kDa) and predicted TS-IPO13 (Ca. 40 kDa).

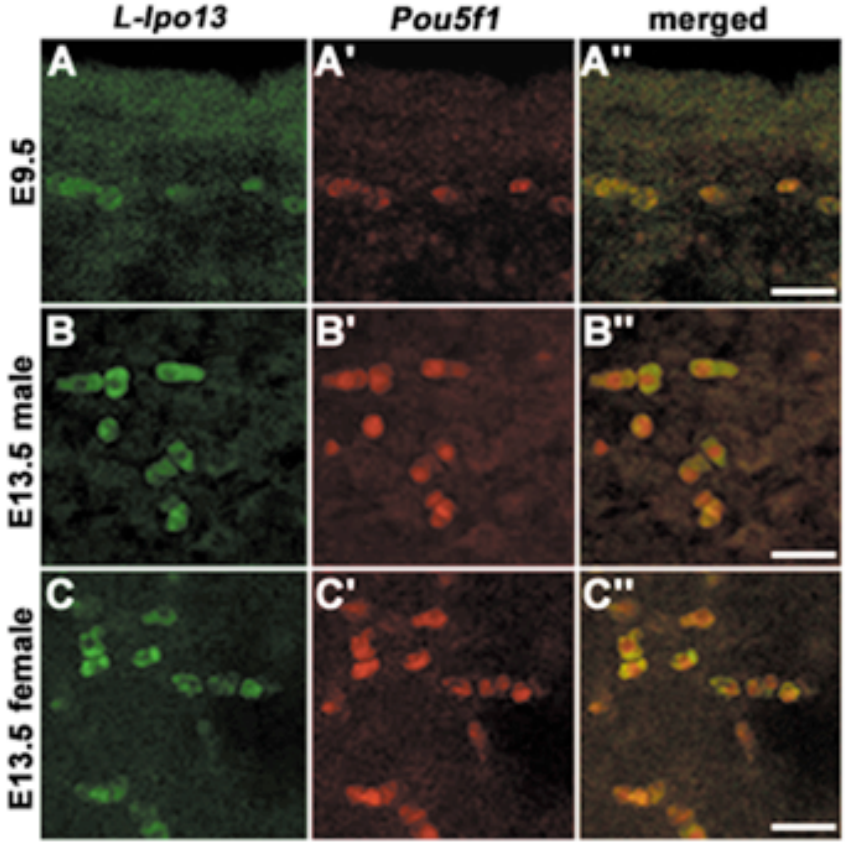

Figure 13 Double in situ hybridization of primordial germ cells
Expression of *Ipo13* is detected in the *Pou5f1*-positivie PGCs in the mesentery of the hindgut of E9.5 embryo (A-A"), and germ cells in the E13.5 fetal testis (male: B-B") and fetal ovary (female: C-C"). Bar:s=20 μm.

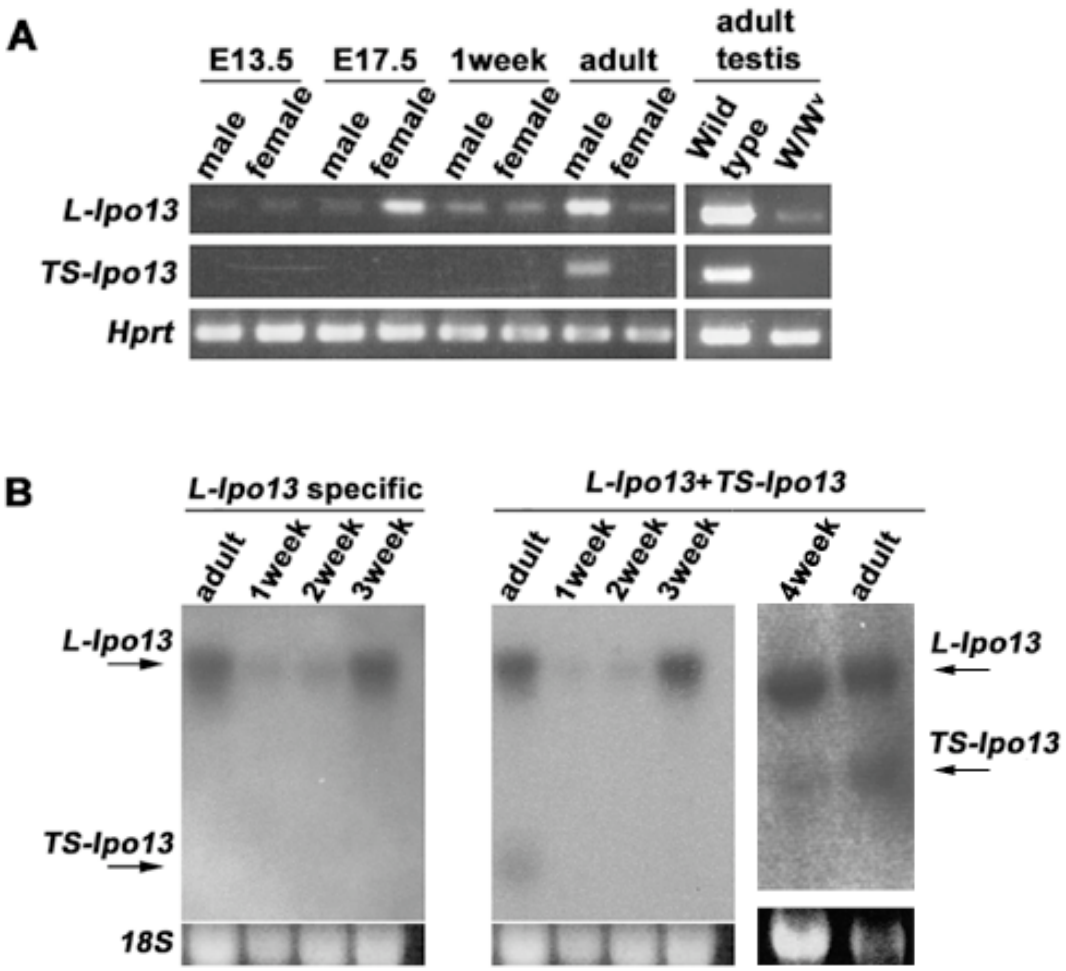

Figure 14 The expression profile of *L-Ipo13* and *TS-Ipo13* transcripts during gonadal development

L-Ipo13 and *TS-Ipo13* expression in fetal (E13.5 and 17.5), neonatal (1week) and adult gonads of both sexes, and in the *W/W*^{v} adult testis that is deficient of spermatogenic cells (A). *Hprt*, loading control for RT-PCR.

L-Ipo13 and *TS-Ipo13* expression in neonatal testes (1-, 2- , 3- and 4-week-old) and adult testis. The 3.4 kb *L-Ipo13* transcripts and the 1.6 kb *TS-Ipo13* are detected by Northern blot (B). *18S*, loading control.

pachytene stage of prophase I of meiosis (**Fig. 14B**). In contrast, *TS-Ipo13* expression is first detected in the 4-week-old testis (**fig. 14B**) and attains the strongest expression in the adult testis (**Fig. 14B**). A low level of expression of *L-Ipo13* and no *TS-Ipo13* transcripts are detected in the testis of the W/W^v mutant mice (**Fig. 14A**). The faint expression of *L- Ipo13* in the mutant testis may be related to the depletion, though not complete absence, of spermatogenic cells (Ohta et al., 2003). These findings strongly suggest that *L-Ipo13* is expressed predominantly in the male germ cells. The pattern of expression of *L-Ipo13* in the meiotic germ cells was examined by *in situ* hybridization on histological preparations of the adult testis. Using *L-Ipo13*-specific L-probe (**Fig. 10**), strong expression of *L-Ipo13* is revealed in the pachytene stage spermatocytes localized immediately next to the spermatogonia (**Fig. 15B-B'** and **15C-C'**), while non-specific signals are found in the outer spaces of seminiferous tubules using control sense probe (**Fig. 15A-A'**). *In situ* hybridization using the C-probe (**Fig. 10**), which recognizes both *L-Ipo13* and *TS-Ipo13* transcripts, revealed no significant difference in the pattern of expression (**Fig. 15D**). To investigate the cell-type that expresses *TS-Ipo13*, *TS-Ipo13* specific probe (75bp of *TS-Ipo13* specific sequence that the position is showed in **Fig. 10**) was used for hybridization, but no specific signals were detected in the adult testis (**Fig. 15E**). *TS-Ipo13* expression is therefore restricted in germ cells at late-pachytene to spermatid stage. In the spermatocytes, localized signals for *Ipo13* ribo-probe can also be detected in the nucleus (**Fig. 15B', 15C', 15D, 17D** and **17F**).

In the female gonads, to elucidate the stage when *L-Ipo13* highest expression commences during oogenesis, RT-PCR is performed on the fetal ovaries of E13.5-20.5

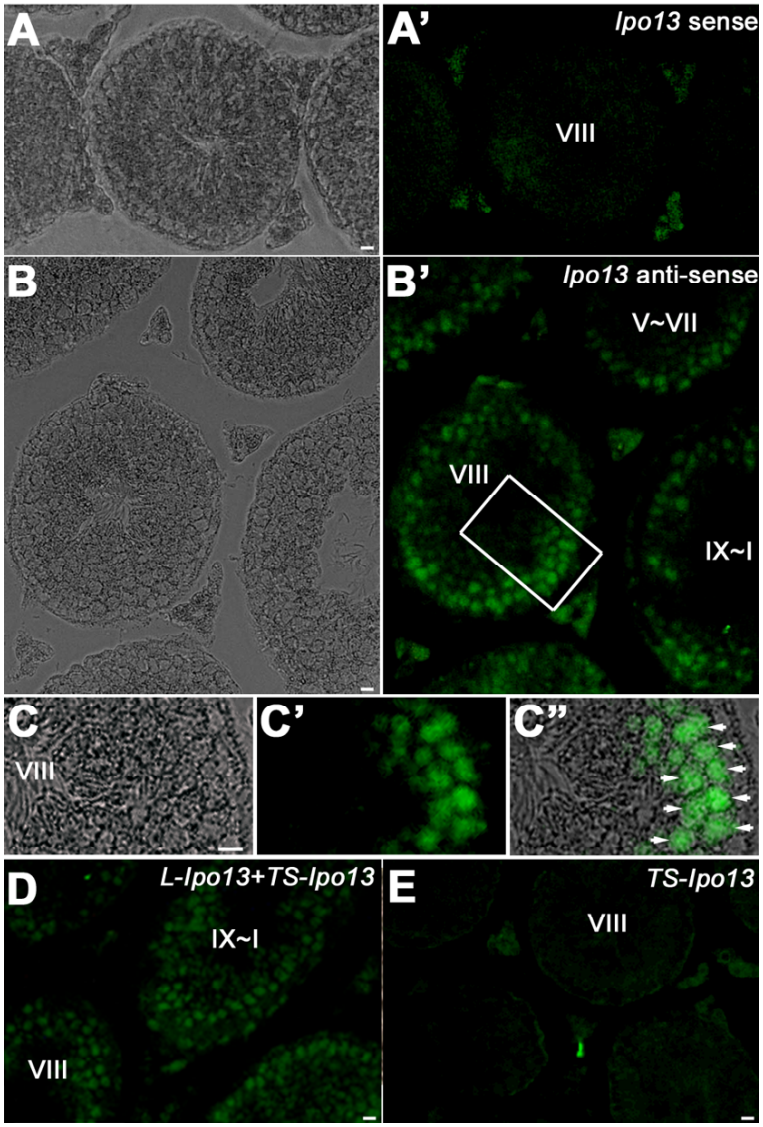

Figure 15 In situ hybridization of *L-Ipo13* in pachytene stage germ cells in testis

A~E: Expression of *Ipo13* transcripts in adult testis. Using with a sense control riboprobe, non-specific signals were found in the connective tissue cells out of the seminiferous tubules (A and A'). *L-Ipo13* specific *L-probe* showed the expression in the primary spermatocytes (B~C'', white arrows, expression is revealed by the green fluorescence produced by the fluorescein-labelled riboprobe). C~C'' is the magnified view of the boxed area in B'. (D) Similar expression pattern was found using C-probe, which detects both *L-Ipo13* and *TS-Ipo13* transcripts, while (E) *TS-Ipo13* specific TS-probe (75bp) did not show any obvious signals. Roman numerals indicate the stage of development of the seminiferous epithelium (Russell et al., 1990). Scale bar: 20 μm.

embryos. Strongest expression of *L-Ipo13* is also detected at E17.5-19.5 ovary where pachytene germ cells are present, and by E20.5 the expression returns to the low E13.5 level (**Fig. 16A**). To confirm the germ cell predominantly expression of *L-Ipo13* in fetal ovary, I performed *in situ* hybridization on E17.5 and 19.5 ovary sections using a fluorescein labeled ribo-probe (L-probe, position showed on **Fig. 10**). *L-Ipo13* is expressed predominantly in the pachytene stage *Ddx4 (Mvh)*-positive oocytes of the E19.5 (**Fig. 16B-B'** and **16C-C'**) and E17.5 fetal ovary (**Fig. 16D-D'''**). In E17.5 and E19.5 ovary which germ cells undergo mid and late-pachytene stage of meiotic progress, according to McClellan et al. (2003).

L-Ipo13 therefore is expressed most strongly in male and female germ cells at the pachytene stage of meiosis I.

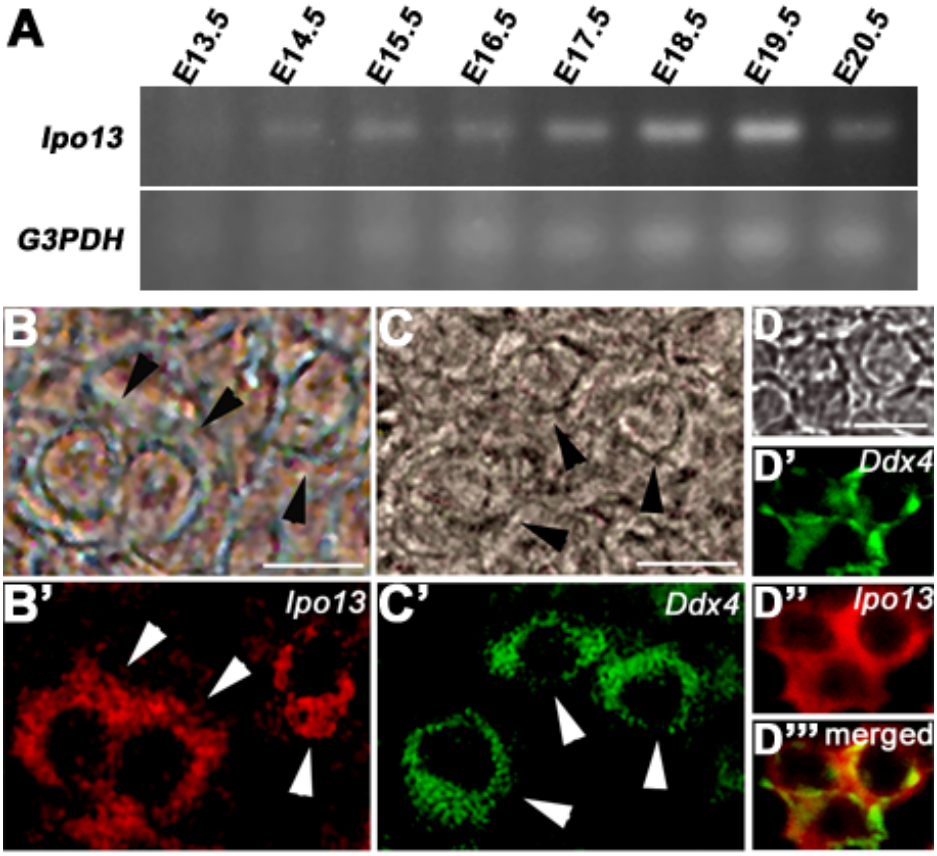

Figure 16 Expression pattern of *Ipo13* in pachytene stage germ cells in ovaries.
A: *Ipo13* expression in fetal (E13.5 ~20.5) ovaries. *G3PDH*, loading control for RT-PCR.

B-D''': Expression of (B') *L-Ipo13* and (C') *Ddx4*/*Mvh* transcripts in oocytes in E19.5 fetal ovary. *L-Ipo13* transcript is detected (D'') in the primary oocytes (*Ddx4*-positive, D') in E17.5 fetal ovary (D''': merged image). B, C, D: bright-field images. Arrowheads indicate either *L-Ipo13*- or *Ddx4*-positive oocytes. Scale bar: 10 μm.

2-ii. Enforced expression assay of *Importin13* in male germ cells

In human, IPO13 is reputed to regulate the nuclear localization of UBC9 (Mingot et al., 2001). In the adult testis, the nuclear localization of UBC9 is found in the pachytene and later stage spermatocytes in the stage specific manner (**Fig. 17A**, **17B-B'** and **17C-C''**). This result suggests that the stage specific expression of *L-Ipo13* may be associated with the regulation of stage specific nuclear localization of UBC9 in the pachytene spermatocytes, which is consistent with previous report of the presence of UBC9 in the synaptonemal complexes (Kovalenko.et al., 1996) at late-pachytene spermatocytes.

I examined if the expression of *L-Ipo13* may coincide with the nuclear localization of UBC9 in a stage-specific manner in the meiotic germ cells by *in situ* hybridization of the *L-Ipo13* and immunostaining of UBC9 in the serial sections of the adult testes. In the pachytene stage spermatocytes that express *L-Ipo13* transcripts (**Fig. 17D** and **17F**), UBC9 protein is widely distributed in the cytoplasm (**Fig. 17E** and **17F'-F''**, white arrows) in the stage V seminiferous tubule. UBC9 shows nuclear localization characteristically in the round spermatids that have down-regulated *L-Ipo13* expression (**Fig. 17F-F''**, black arrows). These results show that elevated expression of *L-Ipo13* in the pachytene stage spermatocytes precedes the nuclear accumulation of the UBC9 protein (**Fig. 17G**).

To further elucidate if L-IPO13 mediates nuclear import of UBC9, the distribution of UBC-MYC fusion protein was examined in GC1 cells (the cell line which were derived from spermatogenic cells; Hofmann et al., 1992) that expressed *L-Ipo13-IRES-GFP*. In cells that expressed L-IPO13 (**Fig. 17H a''**), UBC9-MYC fusion protein was localized predominantly in the nucleus **(Fig. 17H a, a'**, white arrows, see legend for further details).

In contrast, UBC9-MYC was not localized to the nucleus of GC1 cells that expressed the TS-IPO13 (**Fig. 17C b-b"**) and in cells that expressed the IRES-GFP construct that encodes no L-IPO13 (**Fig. 17C c-c"**). No epitope that may cross-react with the anti-MYC antibody were detected in GC1 cells expressing only the GFP (**Fig. 17C d-d"**), suggesting that the immunoreactive protein detected in the L-IPO13 and TS-IPO13 expressing cell is likely to be the UBC9-MYC fusion protein. The expression pattern of *L-Ipo13* and UBC9 in the primary spermatocytes *in vivo* and the effect of *L-Ipo13* expression on the sub-cellular localization of UBC9 in the GC1 cells suggest that the activity of the L-IPO13 influences the nuclear accumulation of a cargo of human IPO13, UBC9, in the germ cells.

To test if the activity of L-Ipo13 might be counteracted by TS-IPO13, GC1 cells were co-transfected with constructs coding the two isoforms separately. As previously shown, UBC9-MYC fusion protein was localized predominantly in the nucleus in the L-IPO13 expressing cells (19/20 = 95%; **Fig. 17I a-a"'**, arrows). In contrast, about 36% of GC1 cells co-expressing L-IPO13 and TS-IPO13 failed to display nuclear localization of UBC9-MYC (**Fig. 17I b-b"'**, arrowheads). Only 64% of cells that co-expressed L-IPO13 and TS-IPO13 showed nuclear localization of UBC9-MYC fusion protein (14/22), as contrasted to about 95% of cells expressing L-IPO13 (significant difference at $P<0.05$ by *Chi*-squared test). This finding showed that L-IPO13 meditated nuclear import of cargo molecules (such as UBC9-MYC fusion protein) may be negatively regulated by the activity of TS-IPO13.

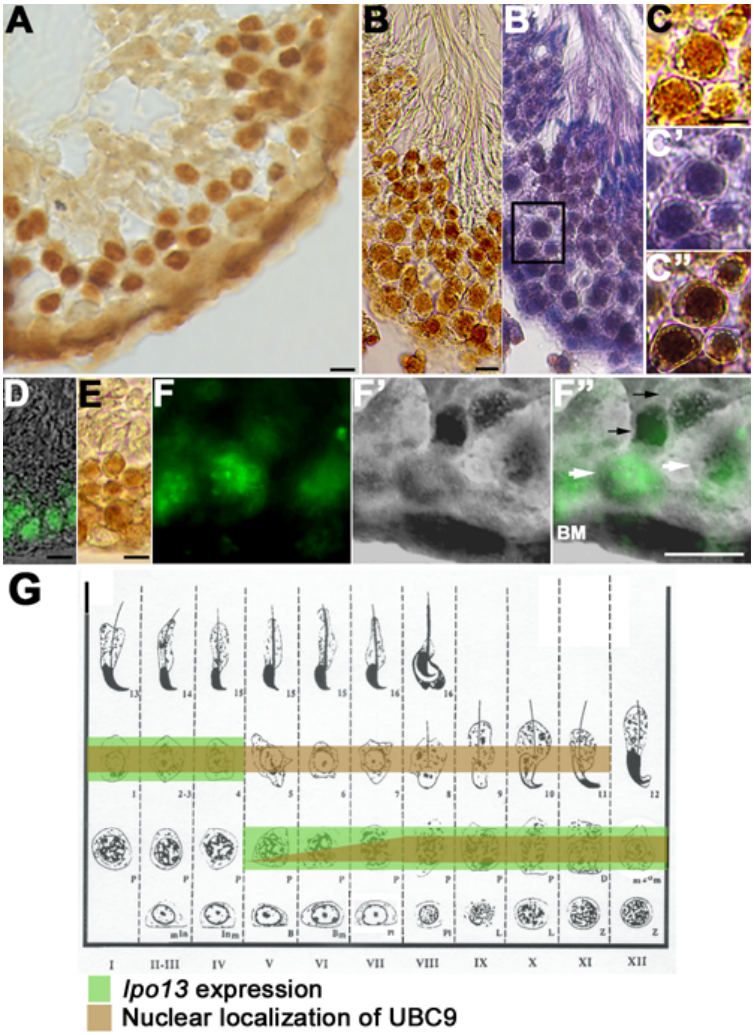
A
B
B'
C
C'
C''
D
E
F
F'
F''
BM
G
I
II-III
IV
V
VI
VII
VIII
IX
X
XI
XII
lpo13 expression
Nuclear localization of UBC9
H
pCMV-Ubc9-Myc
+L-lpo13IRESGFP
+TS-lpo13IRESGFP
+IRESGFP
IRESGFP only
UBC9-MYC
DAPI(nucleus)
GFP+DAPI
a
b
c
d
a'
b'
c'
d'
a''
b''
c''
d''

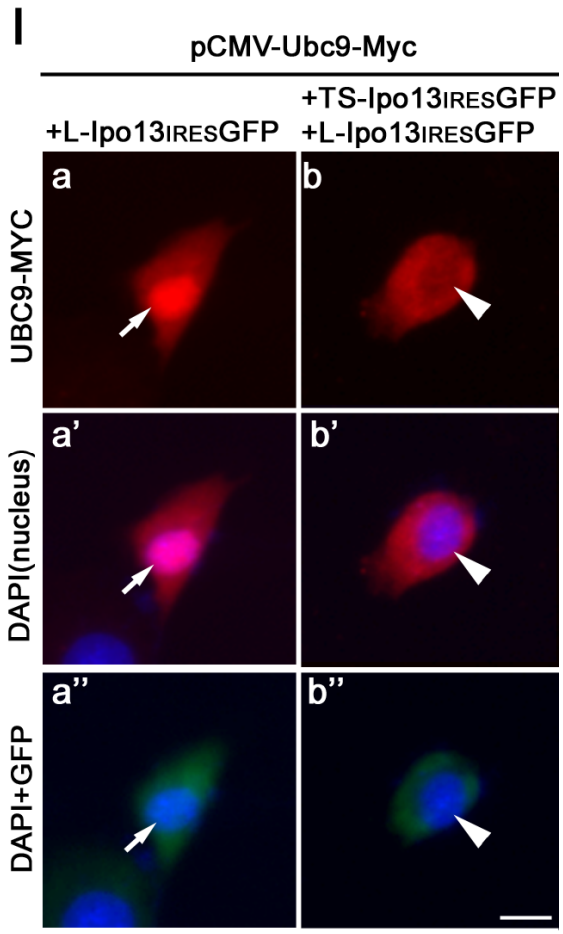
I
pCMV-Ubc9-Myc
+L-Ipo13IRESGFP
+TS-Ipo13IRESGFP
+L-Ipo13IRESGFP
UBC9-MYC
DAPI(nucleus)
DAPI+GFP
a
b
a'
b'
a''
b''

Figure 17 IPO13 mediates nuclear accumulation of UBC9
A-C": The nuclear localization of UBC9 protein in the pachytene-stage primary spermatocytes of the adult testis in the stage VIII seminiferous tubules (immunostaining by anti-UBC9 antibody). B': HE-stained image of B. C-C'' is the magnified view of the boxed area in B'. UBC9 localization (C) was found in nuclei (C': HE-stained) in the spermatocytes (C'': merged).
D-F'': Expression of (D) *L-Ipo13* transcripts and (E) UBC9 in the stage V seminiferous tubules.Non-overlapping distribution of spermatogenic cells (F) displaying expression of *L-Ipo13* mRNA and (F') those showing nuclear accumulation of the UBC9 in the stage V seminiferous tubules (F'': merged image). In early spermatocytes showing strong expression of *L-Ipo13*, UBC9 protein is distributed widely the cytoplasm (marked by white arrows in F'') whereas in round spermatids that ceased to express *L-Ipo13* strongly UBC9 is localized to the nucleus (black arrows in F''). BM, basement membrane.
G: Schematic illustration showing developmental stages of male germ cells expressing *L-Ipo13* and showing nuclear accumulation of UBC9, according to the staging of the seminiferous tubules by Russell et al. (1990).
H: In *L-Ipo13-IRES-EGFP* transfected GC1 cells (a"), UBC9-MYC (produced by expression of the *pCMV-Ubc9-Myc* construct) is accumulated preferentially in the nucleus (a, a'; white arrows in a'). About 50% of the GFP-positive cells showed nuclear localization of UBC9-MYC and the remaining showed both nuclear and cytoplasmic localization. No GFP-expressing cells were found to display only cytoplasmic distribution of UBC9-MYC. In contrast, expression of *TS-Ipo13* (b") did not lead to any nuclear accumulation of UBC9 (b, b'; white arrowhead in b'). The UBC9 protein (c) does not show any nuclear accumulation (white arrowheads in c') when the cells were transfected with the IRES-GFP construct (c"). No other molecules containing the epitope that may be recognized by the anti-MYC antibody was detected (d, d') in cells expressing only the IRES-GFP construct (d"). a-d: red immunofluorescence with anti-MYC antibody; a'-d': DAPI staining for the nucleus merged with a-d; a''-d'': GFP expression in transfected cells merged with a'-d'. Three replicate experiments were performed, and between 60-70 cells were scored in total for each of the four transfection-types. Scale bar: 10 μm
I: In *L-Ipo13-IRES-EGFP* transfected GC1 cells (a"), UBC9-MYC is accumulated preferentially in the nucleus (a, a'; white arrow). In contrast, cells which co-express both *L-Ipo13-IRES-EGFP* and *TS-Ipo13-IRES-EGFP* (b") did not show the nuclear accumulation of UBC9-MYC (8/22; b, b'; white arrowhead). Scale bar: 10 μm

2-iii. Down regulation of *Importin13* leads to delay of meiosis

To further elucidate the role of L-IPO13 in germ cell differentiation, I performed siRNA (short interference RNA) knockdown of *Ipo13* activity in the fetal ovaries cultured *in vitro*, which based on ovary *in vitro* culture system. Oocytes enter the prophase of meiotic division at around E13.5 and reach the pachytene stage at E15.5-19.5 (**Fig 2A**). Staging of oocyte was done based on the nuclear morphology (revealed by DAPI staining) and the synaptonemal complex (anti-SCP3 staining pattern) structure respectively (Schalk et al., 1998; McClellan et al., 2003; Park and Taketo, 2003). The Zygotene/Pachytene (Zy/Pa) stage oocytes have irregularly shaped nucleus, and thick and long strands of synaptonemal complex on the condensed chromatid (**Fig. 18A** Zy/Pa). The mid-pachytene (M-Pa) and late-pachytene (L-Pa) oocytes are identified by the spherical and enlarged nuclei. The M-Pa oocytes show decondensing chromatids which are still decorated with strands of SCP3-positive synaptonemal complex (**Fig. 18A** M-Pa), whereas the L-Pa oocytes show more extensively de-condensed chromatids and clumping of SCP3-positive material (**Fig. 18A** L-Pa). The Pachytene/Diplotene (Pa/Di) stage oocytes have large and spherical nucleus containing completely de-condensed chromatids and one to two clumps of anti-SCP3 antibody stained material (**Fig. 18A** Pa/Di).

The transfection and culture procedures were tested for their impact on the meiotic differentiation of the oocytes in the fetal ovaries cultured *in vitro*. Either electroporation of CMV-GFP vector (**Fig. 18B, a**) or micro-injection of liposome solution of CMV-GFP was localized enforcing vector expression in E15.5 fetal ovary (**Fig. 18B, b**). In contrast, lipofection of siRNA with scrambled sequence tagged by Alexa488 was found to be more

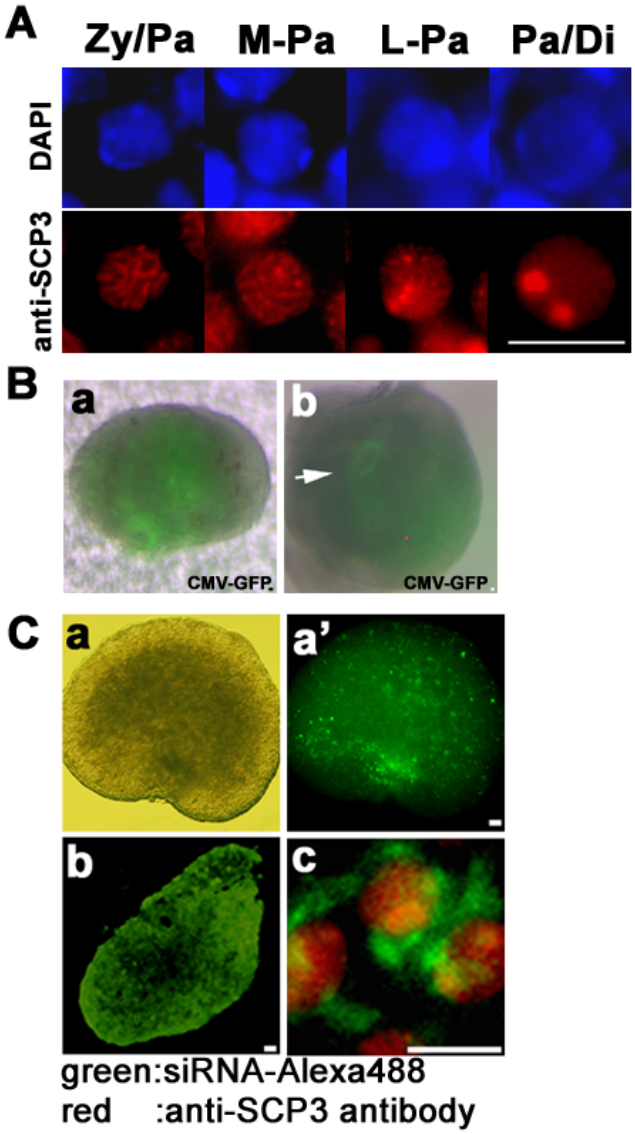

Figure 18 Introduction of transgenes on ovary culture system

A: Staging of oocyte was done based on the morphology of the nuclei (revealed by DAPI staining, blue) and the synaptonemal complex (anti-SCP3 staining pattern, red). **B**: Whole mount view of the cultured fetal ovaries transfected CMV-GFP either (B, a) by the electroporation, or (B, b) by the micro-injection of the lipofection solution. GFP expression showed the tansfection efficiencies on the E15.5 cultured ovaries. **C**: Introduction of siRNA on the E15.5 ovary. Whole mount view of the cultured fetal ovary transfected Alexa488 tagged siRNA by the lipofection (C, a; bright-field image, and b; fluorescence image). The siRNA lipofected and cultured fetal ovary showing (C, a and b) green fluorescence due to the Alexa488 tagged scrambled sequence (SS) siRNA. In frozen section of the cultured fetal ovary (C, c), oocytes are showing (C, d) green fluorescence of siRNA-Alexa488 and red immunofluorescence with anti-SCP3 antibody. Scale bar: 10 μm

wide and efficient than electroporation and micro-injection of liposome solution when the stromal tissues of fetal ovary was exposed microsurgically (see material and method; **Fig. 18C a-b**). In the fetal ovary treated with siRNA with scrambled sequence tagged by Alexa488 at E15.5 and cultured for 3 days *in vitro*, 60-95% (average: ca. 80%) Alexa488 positive oocytes (**Fig. 18C a-b**) also stained positively with anti-SCP3 (synaptonemal complex protein 3) antibody (**Fig. 18C c**). This finding shows that the transfection and culture procedures are efficient and have no impact on the meiotic differentiation of the oocytes.

The role of L-IPO13 in germ cell differentiation was examined by siRNA knock-down of *Ipo13* activity. Two siRNA constructs were used; siRNA#1 and siRNA #2, which are directed to different sequences of the *L-Ipo13* mRNA (**Fig. 10**). Both reagents were found to be effective in the knockdown of L-IPO13: The amount of L-IPO13 protein (about 92 kDa) was significantly reduced in the siRNA-treated ovary when compared to that in fetal ovaries treated with siRNA comprising of a scrambled sequence (SS) (**Fig. 19A a, b**). Consistent with this result, RT-PCR analysis also demonstrated that *L-IPO13* expression level was reduced in siRNA-treated ovary (**Fig. 19A c, d**).

To confirm the impact of *L-IPO13* knockdown on trafficking of cargo molecules, we examined a subcellular localization of UBC9 in the knockdown oocytes. The results showed that a nuclear accumulation of UBC9 (92.5% in control oocytes; **Fig. 19B a and a'**) was impeded in the knockdown oocytes at pachytene stage (67.9% in knockdown oocytes; **Fig. 19B b and b'**; significant difference at $P<0.01$ by *Chi*-squared test. Number of oocytes (n) examined were: control oocytes, n=40; siRNA treated oocytes, n=56). Therefore, it

suggested that knockdown of *L-IPO13* inhibits trafficking of cargo molecule(s) in the meiotic oocytes.

To determine the impact of L-IPO13 knockdown on meiosis, we have examined the relative frequency of meiotic oocytes at different stages of prophase I in the siRNA-treated fetal ovary. Staging of oocyte was done based on the nuclear morphology (revealed by DAPI staining) and the synaptonemal complex (anti-SCP3 staining pattern) respectively (Schalk et al., 1998; McClellan et al., 2003; Park and Taketo, 2003).

In the E15.5 fetal ovary collected at the beginning of the in vitro culture experiment, all oocytes are at the zygotene/pachytene stage (**Fig. 19C** E15.5 *in vivo*). In the E18.5 fetal ovary (**Fig. 19C** E18.5 *in vivo*), the oocytes are at different stages of prophase of meiosis I: 6.1% at Zy/Pa, 40.8% at M-Pa, 20.4% at L-Pa and 32.7% at Pa/Di (**Fig. 19C**). In the untransfected (**Fig, 19C** not transfected) or siRNA treatment control (**Fig. 19C** SS; scrambled sequence) ovaries cultured from E15.5 for 3 days *in vitro* to the equivalent age of E18.5, the distribution of oocytes to the four meiotic prophase I stages were not different from the E18.5 fetal ovary (**Fig. 19C** E18.5 *in vivo*), suggesting that the in vitro culture condition supports normal progression of meiosis, and the lipofection of exogenous RNA have no adverse effect on the differentiation of the oocytes. In marked contrast, fetal ovary treated with either siRNA#1 or siRNA #2 and cultured for the same period after treatment contained about 50% fewer L-Pa stage oocytes that were transfected with the siRNA tagged by the Alexa488. There was a concurrent increase in the proportion of M-Pa oocytes among the meiotic germ cells (**Fig. 19C** siRNA#1; siRNA #2). Knockdown of *L-IPO13* activity therefore impedes the progression of meiosis to the L-Pa phase in about 10-11% of the

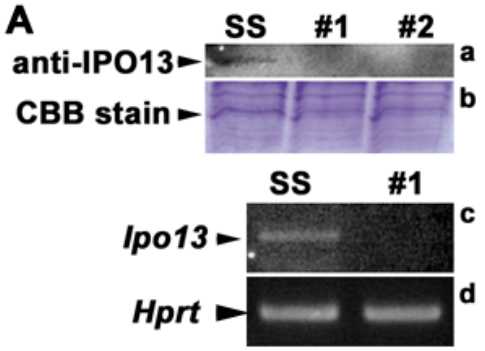

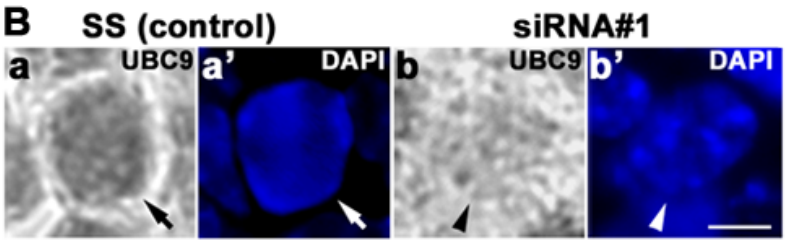

C

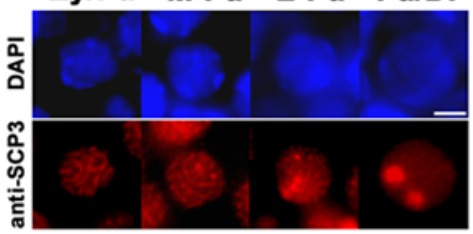

E15.5 (*in vivo*)	100%			
E18.5 (*in vivo*)	6.1%	40.8%	20.4%	32.7%
not transfected	5.9%	41.2%	23.5%	29.4%
SS	6.0%	41.4%	23.3%	29.3%
siRNA#1	5.9%	58.0%	12.6%	23.5%
siRNA#2	3.1%	61.1%	13.0%	22.8%

Figure 19 IPO13 function is required for the progression of prophase I of meiosis during oogenesis

A: The extent of knockdown of IPO13 in fetal ovary treated by siRNA (reagents #1 and #2) relative to the level of protein expression in the control with scrambled sequence siRNA (SS). Western analysis showing reduced amount of IPO13 in the siRNA-treated fetal ovary (a), and the band containing IPO13 as detected by coomassie brilliant blue (CBB) staining also shows reduced amount of protein in the siRNA-treated fetal ovary (b). One ovary (E15.5 + 3 days *in vitro*) was loaded for a each lane. Reduction of *Ipo13* expression was also detected by RT-PCR in the knockdown ovary. c: *Ipo13* expression; d: *Hprt* expression (control).

B: *Ipo13* knockdown inhibits nuclear accumulation of UBC9 in oocytes. Nuclear accumulation of UBC9is impeded in knockdown oocytes (arrow-heads in b and b') but not in SS (arrows in a and a'). Scale bar: 5 μm

C: Four different stages of meiotic prophase: Zygotene/Pachytene (Zy/Pa), Mid-pachytene (M-Pa), Late-pachytene (L-Pa) and Pachytene-Diplotene (Pa/Di).

Zy/Pa: irregularly shaped nuclei, and thick and long strands of SC (synaptonemal complex), M-Pa: spherical nuclei and decondensing chromatid with strands of SC, L-Pa: spherical and enlarged nuclei with decondenced chromatid with clumping of anti-SCP3 stained material, Pa/Di: large spherical nuclei and completely decondenced chromatid with one to two clumps of anti-SCP3 stained material. Scale bar: 5 μm

The tabulated results show the distribution of the siRNA-treated oocytes (identified by the expression of green Alexa488 fluorescence) to the four categories of oocytes at different stages of meiotic prophase I in E15.5 (*in vivo*) fetal ovary (beginning of the experiment) and E18.5 (*in vivo*) fetal ovary and in the cultured ovaries (E15.5+3 days in vitro; equivalent to E18.5) which were not transfected (not transfected) or treated with scrambled sequence (SS) siRNA and the two experimental groups treated by siRNA of siRNA#1 and siRNA#2. There are increases in proportion of mid-pachytene stage oocyte and corresponding decreases in late-pachytene and pachyene-diplotene stage oocytes in the two siRNA treatment groups (significant difference between SS and siRNA#1 or siRNA#2 at $P<0.05$ by *Chi*-squared test). Three replicate experiments were performed for the not-transfected, SS, siRNA#1 and siRNA#2 groups and results of each experiment were obtained from three cultured specimens. Three samples of fetal ovaries each of E15.5 (*in vivo*) and E18.5 (*in vivo*) were scored for the number of germ cells at different meiotic stages. Numbers of oocytes (n) examined were: E15.5 (*in vivo*), n=65; E18.5 (*in vivo*), n=49; not transfected, n=51; SS, n=116: siRNA#1, n=119; siRNA #2, n=162.

oocytes. This finding therefore implicates a role of L-IPO13 in regulating the progression through the pachytene stage of prophase I of meiosis.

3. DISCUSSION

Expression of *Importin13* accompanies the progression through the pachytene stage of meiosis during gametogenesis

In general, *Importin-β* family genes are not known to be expressed in lineage- or stage-specific pattern. The present study showed the identification of two transcripts of the mouse *Ipo13* gene, which are encoded as *L-Ipo13* and *TS-Ipo13*, and demonstrated that *L-Ipo13* is expressed predominantly in the migratory PGCs and in the germ cells that colonize the E13.5 fetal gonad of both sexes. *L-Ipo13* expression is elevated fetal ovary when the germ cells enter into meiosis, and the expression is detected predominantly in the pachytene stage oocytes. The elevated expression is detected at E17.5-19.5 ovary where pachytene germ cells are present. In the male mouse, *L-Ipo13* is strongly expressed in the spermatocytes as they enter into the pachytene stage of the prophase I of meiosis and is down-regulated in germ cells past the pachytene stage in adult testis. The temporal relationship of the stage-specific expression of *L-Ipo13* in the pachytene stage primary spermatocytes and primary oocytes is consistent with a role of L-IPO13 in the regulation of progression of the prophase I of meiosis during gametogenesis.

Members of Importin family mediate nuclear transport of molecular cargoes depending on the gradient of GTPase activity of Ras-related nuclear protein (Ran-GTPase). Members of this family are accountable for the recognition of the majority of nuclear import and export cargoes through the nuclear pore complex (NPC) to shuttle between nuclear and cytoplasm by the RanGTP gradient rule, which RanGTP gradient across the nuclear envelop, with a high concentration of RanGTP molecules and low levels in the cytoplasm controls

cargo binding and release (Strom and Weis, 2001;Weis, 2003). The differential expression of *L-Ipo13* during meiosis of the male germ cell may be functionally linked to the cargo delivery activity of the Ran-GTPase genes, *Ran*/M1 or *Ran*/M2, that are also expressed in the pachytene spermatocytes and round spermatids (Lopez-Casas et al., 2003).

In *Drosophila* and *C. elegans*, *Importin-α* family genes are shown to have a function in meiotic germ cell differentiation, but the expression of thos *Importin-α* genes are not specific to the stages when they show the critical functions in germ cells (Geles and Adam 2001; Giarre et al., 2002; Gorjanacz et al., 2002; Mason et al., 2002). In mouse spermatogenesis, the regulation of the nuclear-cytoplasmic transport is proposed to be critical for germ cell differentiation, but such transporting machinery is still unclear (Hogarth et al., 2005). Present study on L-IPO13 provides a novel clue in understanding the regulatory mechanisms of meiotic germ cell differentiation by the nuclear-cytoplasmic transport machinery in the stage-specific manner in mice. A compelling indication of the critical function of L-IPO13 in the progression of prophase I of meiosis is shown by the delay in the transition from mid- to late-pachytene of female germ cells in the Ipo13-siRNA treated fetal mouse ovaries.

The two forms of Importin13 protein; may have different functions in spermatogenesis

Importin-β family proteins bind RanGTP via the amino-terminal domain and cargo via the carboxy-terminal domain, and a nuclear import cargo can bind C-terminal domain when these proteins do not associate to RanGTP that concentrated in nucleus (Strom and Weis, 2001). The putative peptide encoded by *TS-Ipo13* transcript lacks the N-terminal RanGTP-

binding domain but has the C-terminal cargo-binding domain of the full-length *L-Ipo13* transcript. Members of *Importin-β* family are known to mediate the transport of molecular cargoes between the nucleus and the cytoplasm in response to a graded Ran-GTPase activity which regulates the kinetics of binding and release of the cargoes is mediated by the activity of the RanGTP-binding domains in the N-terminal part of the Importin-β protein. The response to Ran-GTPase activity leads to the coupling of Importing with the cargo via the carboxy-terminal domain (Strom and Weis, 2001). Consistent with this concept, protein pull-down assay has revealed that rat IPO13 protein is coupled to the functional RanGTP-binding domain in the N-terminal amino acids 1-488 fragment, but not in the C-terminal 489-963 amino acids fragment (Tao et al., 2004). The putative peptide encoded by *TS-Ipo13* transcript lacks the RanGTP-binding domain encoded by the N-terminal exon 1-6 sequences of the full-length *L-Ipo13* transcript. In the HeLa cells, the fusion protein encoded by the C-terminal fragment of rat IPO13 protein tagged with EYFP is confined primarily to cytoplasm, while the EYFP-tagged full-length protein is distributed to both the nucleus and the cytoplasm (Tao et al., 2004), suggesting that TS-IPO13 might therefore be unable to respond to RanGTP activity due to the absence of binding domain for RanGTP. It is not known if the lack of RanGTP binding domain prohibits the trafficking of TS-IPO13 to the nucleus or disables the off-loading of the cargo from TS-IPO13 while it is in the nucleus. However, it has been shown that for Importin-β family protein, binding of the to C-terminal domain of the protein can occur even in the absence of any interaction with RanGTP (Strom and Weis, 2001). Definitive evidence for the binding activity of TS-IPO13 to cargo molecules is not available yet. Nevertheless, the end-result is that the cargo, such as UBC9, cannot be imported to the

nucleus in the presence of TS-IPO13, as revealed by the lower frequency of nuclear accumulation of UBC9-MYC in GC1 cells co-expressing TS-IPO13 and L-IPO13. In view of the different effect of TS-IPO13 and L-IPO13 on the nucleo-cytoplasmic distribution of UBC9, it may be inferred that TS-IPO13 and L-IPO13 proteins function differently in germ cells during spermatogenesis. It is likely that TS-IPO13 may act as a dominant negative regulator of the L-IPO13 nuclear import activity by binding with cargo molecules in the cytoplasm. The switch in the mode of trafficking of cargo may be accomplished by changing the relative amount of the two isoforms of IPO13 via the utilization of different transcription start sites. The modulation of the nuclear import activity of IPO13 via the interaction of the native protein and the dominant negative isoform highlighted a heretofore unrecognized paradigm for the regulation of Importin function.

UBC9 is a cargo of L-IPO13 in the mouse germ cells

In the male germ cells, expression of the *L-Ipo13* mRNA in the pachytene spermatocytes precedes the accumulation of UBC9 in the nucleus of the late-pachytene-diplotene spermatocyte, when presumably the L-IPO13 is synthesized. UBC9 is a member of the ubiquitin-conjugating E2 enzymes, which regulate post-transcriptional modification or degradation of target proteins via the ubiquitin-dependent activity (Melchior, 2000; Seeler and Dejean, 2003). Loss of *Ubc9* in the mouse embryo is associated with major chromosome condensation and segregation defects in blastocysts (Nacerddine et al., 2005) which is consistent with a critical role of UBC9 in regulating chromosome dynamics. UBC9 protein is a known cargo of human IPO13 and expression of human IPO13 alone is sufficient to drive

nuclear accumulation of UBC9 in HeLa cells. This effect on UBC9 localization cannot be produced by Importin−β, -5, -7, or the α/β heterodimer or other forms of transportin (Mingot et al., 2001). In contrast to other Importing-β family protein, IPO13 mediates import in and export without any requirement to partner with Importin-α (Mingot et al., 2001).

Recently, human ubiquitin-conjugating class III E2 enzymes, UbcM2, UbcH6 and UBE2E2, were shown to be imported into nucleus by Importin-11 (IPO11). This is accomplished in an ubiquitin activation-dependent manner, such that only the ubiquitin-loaded form efficiently binds to IPO11 (Plafker et al., 2004). However, in contrast to the interaction of IPO11 and UbcM2 (Plafker et al., 2004), a robust interaction was detected between recombinant IPO13 and non-ubiquitin-loaded form of UBC9 (Mingot et al., 2001). This may suggest that interaction of UBC9 and IPO13 is not dependent on the ubiquitin activation of UBC9.

In *Drosophila,* mutations of *lesswright* (*lwr*/*Ubc9)* suppress the non-disjunction and the cytological defects that affect spindle formation in the female meiotic germ cells, suggesting that LWR plays a role in the dissociation of homologous sequences in the heterochromatic regions of the chromosome at the end of meiotic prophase I (Apionishev et al., 2001). In the mouse, UBC9 protein, which is localized at the synaptonemal complex, interacts with the Rad51 DNA recombination/repair enzyme and co-localizes with this enzyme in the synaptomenal complexes of late-pachytene spermatocytes (Kovalenko.et al., 1996).

Recently, other cargoes carried by IPO13 have been identified: they include the NF-YB/NF-YC heterodimeric transcriptional activator (Kahle et al., 2005) and the paired-type

homeodomain transcriptional factor PAX6, PAX3 and CRX (Ploski et al., 2004). Further identification and characterization of cargo molecules of L-IPO13 in meiotic germ cells is still remained.

In summary, *L-Ipo13* expression is up-regulated at the pachytene stage in the prophase of meiosis I, and the activity of L-IPO13 protein mediates the nuclear localization of UBC9 in the stage specific manner in meiotic germ cells during the gametogenesis. In the female germ cells, L-IPO13 activity is required for progression through the pachytene stage of prophase I of meiosis. These findings imply that the stage specific elevation of *L-Ipo13* expression may be a trigger of nuclear import of cargoes, which are essential for regulating meiosis.

Chapter V Region-specific genetic activity at the stage of PGC formation

1. INTRODUCTION

Lineage analysis of the pre- to early-streak (E6.0-6.5) mouse embryo has revealed that precursors of the primordial germ cells (PGCs) are localized in the proximal region of the epiblast (Lawson and Hage, 1994; Tam and Zhou, 1996).

It is known that certain molecular activities, which are specifically expressed in proximal epiblast of the pre-gastrulating embryo. Little is known about the region-specific gene activity that may influence gem cell formation. Prior to gastrulation, *Ifitm3* is expressed widely in the population of proximal epiblast cells where PGC precursors reside. During gastrulation, expression of *Ifitm3* is progressively restricted to the cluster of putative PGC precursors at the base of the allantoic bud. *Ifitm1* is also expressed in the cluster of putative PGC precursors begins in mid- to late-streak-stage embryos (Tanaka and Matsui, 2002; Saitou et al., 2002; Lange et al., 2003; Tanaka et al., 2004). However, knock-down of *Ifitm1* activity in the embryo does not seem to affect PGC formation (Lickert et al., 2005), and the impact of loss of *Ifitm3* function is yet unknown. In view of the lack of information on the molecular mechanisms of PGC formation, it would be worthwhile to identify additional genes that display regionalized expression in the epiblast containing the PGC precursors. In this chapter, the isolation of the region-specific genes that are expressed in the proximal epiblast of the pre-gastrulating embryo was described.

2. RESULTS

cDNA pool synthesis and the subtraction procedure were according to the method by Shimono and Behringer (1999). First-strand cDNAs were synthesized from about fifty cells of dissected proximal epiblast and distal epiblat of the E6.25 embryo with the addition of Poly-d(A) onto 3' end of the cDNA by terminal transferase (Roche), and then the cDNAs were amplified by PCR with poly-d(T) containing primer. PCR-based subtraction was carried out 2 times to generate a proximal epiblast-specific subtracted cDNA library. To validate the experimental procedure, analysis of the subtracted cDNA libraries revealed that *Ifitm3* display proximal-specific expression (**Fig. 20**), as predicted by the pattern of gene expression (Saitou et al., 2002; Tanaka and Matsui, 2002).

Clones from the 2nd subtracted library were screened by Southern blot hybridization using two probes: unsubtracted proximal and distal epiblast cDNAs. To further verify whether the positive clones were specifically expressed in proximal epiblast, positive clones were used as probes for Southern blots of cDNA pools of proximal epiblast and distal epiblast. Screening of 500 clones of the subtracted cDNA library indicated 8 cDNA fragments that are differentially expressed in the cDNA pool of the proximal epiblast tissue (**Fig. 20A**). Among the 8 genes, two known genes, which are encode *plectin* (*Plec1)* and *mitochondria-specific thioredoxin-2* (*Txn-2*), has been validated their regionalized expression by whole mount *in situ* hybridization (**Fig. 20B**).

A

Clone No.	gene name	NCBI accession No.
#16	Mrvldc2	BC049919
#34	Similar to Rat Pairbp1	NM_145086
#38	α-NAC	NM_01360 or U22151
#58	U2 snRNP-A	AF230356
#83	protein phosphatase 2A regulatory subunit B	BC006626
#88	Similar to prostate tumor over expressed gene1	BC038159
#100	Txn-2	NM_019913
#388	Plec1	BC024074

B

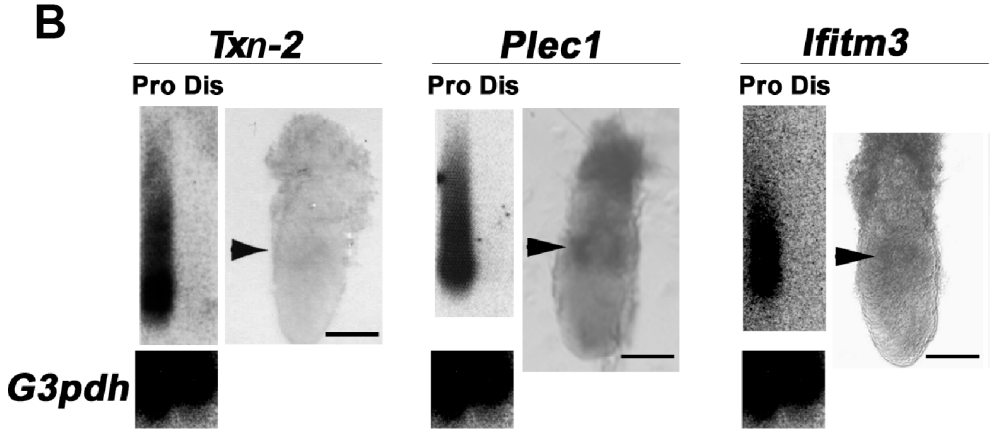

Figure 20 Subtractive screening between the proximal and the distal epiblasts
Eight candidate genes are identified from the screening of 500 cDNA clones of the subtractive cDNA library (A). *Txn -2* and *Plec-1* are shown the expression in the proximal epiblast at the pre-gastrulation by whole mount *in situ* hybridization (B). Pictures of *Ifitm-3* modified from figure.5 in Tanaka and Matsui, 2002.
Bars=100μm.

3. DISCUSSION

Two candidate genes showed regionalized expression in the proximal epiblast of E6.25 embryos, where PGC precursors are localized. *Plec1* encodes the versatile cytoskeletal linker protein, and has an important role in maintaining the structural integrity of diverse cells and tissues (Wiche, 1998). The *Plec1* null mice died 2-3 days after birth exhibiting skin blistering caused by degeneration of keratinocytes (Andra et al., 1997). *Txn-2* is a mitchondria specific member of the thioredoxin superfamily, which encodes redox protein and regulates the redox state (Tanaka et al., 2002). *Txn-2* homozygous mutant embryos are shown embryonic lethal after implantation at around E10.5. The mutant embryos displayed open anterior neural tube and elevated apoptosis (Nonn et al., 2003). The potential function of *Plec-1* and *Txn-2* activity in germ cell formation has yet been investigated.

Chapter VI GENERAL DISCUSSION

1) Search for germ-cell specific molecular factors

Several genes are identified that are specifically expressed in germ cells during early mouse development. These genes are categorized into four groups by their potential functions in A) germ cell-lineage-restriction, B) pluripotency of PGCs, C) migratory PGC differentiation, and D) germ cell differentiation in gonad (**Fig. 21**). Interestingly, some genes, which are known to express in ICM, ES cells and EG cells, are also expressed in PGCs.

In the gastrulating embryo, it has shown that *Ifitm3* expressed in population of proximal epiblast cells, which may be activated in response to BMP4 signaling (Saitou et al., 2002; Tanaka and Matsui, 2002; Tanaka et al., 2004). *Prdm1*-expressing PGC precursors are induced amongst proximal epiblast cells (Ohinata et al., 2005). The relationship between cell populations that express *Prdm1*, *Ifitm3* and genes that were differentially expressed in the proximal epiblast (Chapter V) is unclear.

Prior to PGC formation, expression of *Nanog* and *Dppa3*, which is known to be expressed in ICM and ES cells and EG cells, is down-regulated in the entire epiblast, and PGCs re-acquire the expression after the PGC formation at E7.5 (Saitou et al, 2002; Sato et al., 2002; Yamaguchi et al., 2005). Promoter analysis of *Pou5f1* revealed that transcriptional activity of *Pou5f1* switched through usage of enhancer elements: the proximal enhancer drives the expression in the epiblast, whereas the distal enhancer is for the expression in the ICM and PGCs (Yeom et al., 1996). *Pou5f1* and *Nanog* are known to be involved in the maintenance of pluripotency of ICM, ES cells and EG cells, and predicted to be involved in

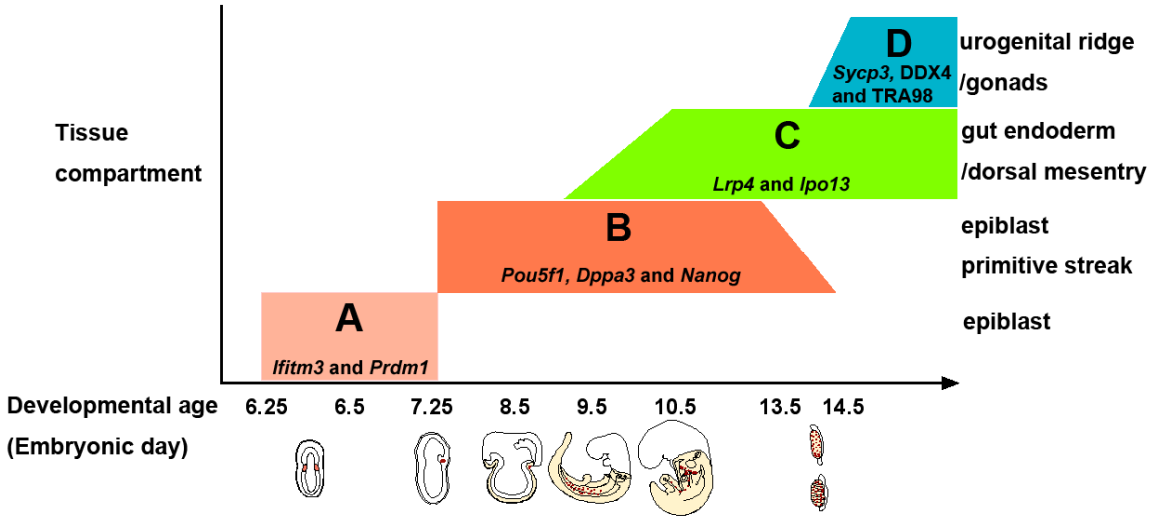

Figure 21 Schematic of mouse germ cell developmental gene expression profile
Ifitm3 and *Prdm1* positive PGC precursors are observed in proximal epiblast (A). The pluripotency of PGCs is associated with the expression of *Pou5f1*, *Dppa3* and *Nanog* (B). In migratory PGC, *Lrp4* and *Ipo13* are expressed (C). On germ cell differentiation after homing of PGCs in gonad, the expression of *Akp3*, *Pou5f1*, *Dppa3* and *Nanog* is down regulated. *Sycp3* expression is up regulated in germ cells in female gonads, and DDX4 expression is observed in both sexes of germ cells. TRA98 antigen is also observed in germ cells in male gonads (D).

the potential function in the maintenance of pluripotency of PGCs. In contrast, two genes that were studied for this project, *Lrp4* and *Ipo13*, are expressed in PGCs, but not in ICM, epiblast, ES cells and EG cells. Therefore, *Lrp4* and *Ipo13* are a one of the PGC specific property that distinguishes germ cells from stem cells at the migratory stage.

2) Germ-cell-specific molecules in migratory PGCs

After entry of PGCs into the genital ridge, PGCs start to show the expression of specific genes, i.e., meiosis-associated genes, and differentiate into gametes depending on the sex of the embryonic gonad (McLaren, 2003). Expression of TRA98 antigen is known to be found in male germ cells from E12.5 (Tanaka et al., 1997). Meiotic-germ-cell-specific *Sycp3* expression is up-regulated at around E13.5 in germ cells in female gonads (Chuma and Nakatsuji, 2001). Germ-cell-specific DDX4 expression also begins to be found in germ cells in the genital ridges in both sexes (Fujiwara et al., 1994; Toyooka et al., 2000). DDX4 has been shown to influence germ cell proliferation in male embryonic gonads (Tanaka et al., 2000). Expression of mouse *Dazl* homolog is first found in the post-migratory PGCs in the E11.5 embryonic gonad, which gene activity seems to be required for development and survival of male germ cells in the embryonic gonad in mice of the inbred C57/BL/6 background (Lin and Page, 2005). In contrast, *Lrp4* and *Ipo13* are novel germ-cell-specific genes which were expressed in migratory PGCs before the entry into the genital ridge.

3) Wnt signaling and the derivation of EG cells

Pou5f1 and *Nanog* are known to be involved in the maintenance of pluripotency of

ICM, and ES cells and EG cells. Expression of those genes in PGCs is therefore consistent with the potential of PGC to form EG cells under culture conditions. *Pou5f1* and *Nanog* expression is down-regulated in germ cells in the female embryonic gonad at around E13.5~15.5 and in the spermatocytes in the testis respectively (Pesce et al., 1998; Yamaguchi et al., 2005). Consistent with the changes in the genetic activity, the efficiency of the derivation of EG cells from E12.5 PGCs is much lower than one from E8.5 PGCs, and the germ cells from the E15.5 gonads did not give rise to EG cell lines under the culture conditions (Labosky et al., 1994). The down-regulation of the stem-cell-specific genes, and other molecule(s) may have direct implication on ability of the derivation of EG cells. In ES cells, active Wnt-signaling plays a crucial role in the self-renewal and maintenance of pluripotency (Sato et al., 2004). In mouse germ cell development, little is known about the role of Wnt-signaling. A postmeiotic loss of oocytes was found in the *Wnt-4* deficient gonad (Vainio et al., 1999) and a lack of *Pten*, which is involved in the suppression of Wnt-signaling pathway in part, in germ cells leads to enhance an efficiency of EG cell derivation (Kimura et al., 2003). *Lrp4* expression is first detected in migratory PGCs in the dorsal mesentery at E8.5~9.5 (Chapter III). *Lrp4* gene activity may suppress PGC self-renewal by modulating of Wnt-signaling in germ cells and thereby induces cell differentiation. This may have bearing to the lower efficiency in deriving EG cells from E12.5 *Lrp4*-expressing PGCs than the E8.5 PGCs (Labosky et al., 1994). It would be informative to test if *Lrp4* gene activity may be correlated with potency of EG formation.

4) Nucleo-cytoplasmic traffic and L-IPO13

This study on the *Ipo13* gene activity in germ cells highlighted a mechanism of the nucleo-cytoplasmic transport that regulates cell differentiation in the meiotic germ cells. For understanding L-IPO13 function in the nucleo-cytoplasmic trafficking in the meiosis of germ cells, it is important to characterize the cargo molecules transported by the Importin molecules. One of the known cargo molecules of human IPO13 is MGN, human homolog of *Drosophila mago-nashi* (Mingot et al., 2001), which gene activity is required for germ cell formation in *Drosophila* (Boswell et al., 1991). However, human *MGN* homolog showed a ubiquitous expression pattern in adult tissues. The potential function of mammalian *mago-nashi* homolog in germ cells is not known (Zhao et al., 1998).

5) Regulation of Importin13 function

This study on *Ipo13* gene activity in germ cells also highlighted potential regulatory mechanisms of Importin function in the nucleo-cytoplasmic trafficking, which is so for unrecognized. Temporal expression of *L-Ipo13* in germ cells mediated nuclear accumulation of UBC9, which is required for meiotic differentiation in mice, in contrast to the non-specific expression of Importin-α proteins in *Drosophila* and *C. elegans* to the stages when they show the critical functions in germ cells (Geles and Adam 2001; Giarre et al., 2002; Gorjanacz et al., 2002; Mason et al., 2002). Furthermore, TS-IPO13 and L-IPO13 proteins function differently in germ cells during spermatogenesis. It is likely that TS-IPO13 may act as a dominant negative regulator of the L-IPO13 nuclear import activity by binding with cargo molecules in the cytoplasm. The switch in the mode of trafficking of cargo may be accomplished by changing the relative amount of the two isoforms of IPO13 via the

utilization of different transcription start sites. It is known that some members of Importin family proteins appear to lack Ran-GTP binding domain, but their function in the nucleo-cytoplasmic trafficking are still unclear. The modulation of the nuclear import activity of IPO13 via the interaction of the native protein and the dominant negative isoform highlighted a heretofore unrecognized paradigm for the regulation of Importin function. Further elucidation of the functional relationship with *TS-Ipo13* and *L-IPO13* in the nucleo-cytoplasmic trafficking will shed a light on understanding the regulatory mechanisms of importin function in the cell differentiation.

Chapter VII MATERIALS AND METHODS

Collection of embryos

Embryos were collected from pregnant mice of ICR x B6D2F1 or ARC/S strain. The use of animal in Children's Medical Research Institute is approved by the Animal Care and Ethics Committee (ACEC) of the Children's Medical Research Institute and the Children's Hospital at Westmead under ACEC project 138. E6.5 to 20.5 embryos, and newborn and adult (more than 6-week-old) gonads were dissected in Dulbecco's modified Eagle medium (DMEM) supplemented with 10% calf serum or in phosphate buffered (PB)-1 medium.

Northern Blot

Total RNA was extracted by using either RNeasy (QIAGEN) or ISOGEN (Nippongene) from several tissues, i.e., testis, ovary, brain, liver and kidney of adult mice (more than 8-weeks), and male and female gonads of different the developmental stages. ES cells (D3) and EG cells (EG1) were cultured on STO feeder cells. Cells were trypsinized and total RNAs were isolated using ISOGEN reagents (Nippongene). For the northern blot analysis, 40 μg of total RNA of ES cells, EG cells and STO cells, 20 μg of total RNA of adult tissues, and 10 μg of total RNA of ovaries and testes were loaded on each lane and transferred to a Hybond-N^+ membrane (Amersham). The P2 probe corresponding to a 3'-UTR region of *Lrp4* (829bp; from 6530bp to 7302bp) was used for the hybridization (Fig. 4B). Hybridization with a 416bp PCR fragment of *Gdph* (from 809bp to 1224bp) provided the internal control. The genomic regions that correspond to positions of the cDNA clone #B94, the L-probe for *L-Ipo13* mRNA and C-probe for both *L-Ipo13* and *TS-Ipo13* mRNA were shown in Fig.10. For the hybridization, the membrane was incubated with the ^{32}P-labeled probe in 50% formamide hybridization buffer at 42°C for 16 hours, and the membrane was washed in 0.2X standard saline citrate (SSC) containing 0.1% SDS at 65°C for 20 minutes twice.

RT-PCR

Poly-A RNAs were extracted using Micro Fast Track mRNA purification kit (Invitrogen) from blastocysts, E9.5 dorsal mesentery and E13.5 fetal gonads. Total RNAs were extracted using RNeasy (QIAGEN) from adult tissues. Reverse transcription was carried out using 0.2 μg mRNA using Superscript II (Invitrogen). PCR amplification was performed using Ex-taq system (Takara) or Taq DNA Polymerase (Roche). PCR amplification was performed for *Lrp4* with 33 cycles of 1 minute at 94 °C, 1 minute at 55 °C and 1 minute at 72 °C. PCR

amplification of *Hprt* was performed with 25 cycles of 1 minute at 94 °C, 1 minute at 60 °C and 1 minute at 72 °C. PCR amplification was performed with 22 cycles for *Gdph* and 28 cycles for *Pou5f1* of 1 minute at 94 °C, 1 minute at 58 °C and 1 minute at 72 °C. PCR amplifications were performed with 35 cycles for *L-Ipo13,* 45 cycles for *TS-Ipo13* and 25 cycles for *Hprt* of 1 minute at 94°C, 1 minute at 60C°, and 1 minute at 72°C, respectively. The PCR products logarithmically increased with the cycles examined, and the products were verified by sequencing. Primer sets for the PCR amplification were:

Lrp4; 5'-cagtgaagatgtaaagtgg-3' and 5'-atgcctggctgctgatctctg-3'.

Gdph; 5'-acatcaagaaggtggtgaagc-3' and 5'-ggtagttatttcaagcgacgt-3'.

Hprt; 5'-ggatttgaaattccagacaag-3' and 5'-gcatttaaaaggaactgttgac-3'.

Pou5f1; 5'-tcgagtatggttctgtaaccg-3' and 5'-aatgatgagtgacagacaggc-3'.

L-Ipo13, L1: 5'-catggcatctgccgtattgc-3' and L2: 5'-tgcatcagccacatgcactg-3'.

TS-Ipo13, TS1: 5'-atcctgattccctctgccctc-3' and TS2: 5'-gcaggttcttcaggatctcc-3'.

The corresponding genomic positions of the primer sets for *Lrp4* and *Ipo13* are shown in Fig 4B and Fig. 10 respectively.

Rapid amplification of cDNA ends (RACE)

5' and 3' RACE were performed by using Marathon cDNA amplification kit according to the manufacturer's instruction (Clontech). First strand cDNAs were synthesized from a poly(A) RNA, which was purified using Oligotex-dT30 (Roche) from adult testis total RNA. To confirm the expression of two RACE products as intact transcripts, end-to-end RT-PCR was carried out with *L-Ipo13* or *TS-Ipo13* specific primer sets. Sequences of the primer sets are listed below and the corresponding genomic positions are shown in Fig 10.

L-Ipo13, L3: 5'-agatggagcggcgggaggag-3' and L4: 5'-ctcagtagtcagctgtgtag-3'.

TS-Ipo13, TS1: 5'-atcctgattccctctgccctc-3' and L4: 5'-ctcagtagtcagctgtgtag-3'.

Sample preparation for *in situ* hybridization and histochemistry

Embryos and adult tissues were fixed with 4% paraformaldehyde (PFA) in phosphate buffer saline (PBS). Testes were collected from adult mice that were anaesthetized and perfused by 4% PFA in PBS for fixation of tissues. After dehydration in graded ethanol-series, tissue specimens were cleared in xylene and embedded in paraffin (Paraplast; Oxford labware), and 10 μm section were prepared for *in situ* hybridization and immunohistochemistry.

For the whole-mount *in situ* hybridization, E6.5 to 9.5 embryos and the genital ridge of E10.5

to E13.5 embryos were dissected and fixed with 4% PFA in PBS containing 1% Tween-20 (Sigma) overnight. After dehydration in graded methanol-series, tissue specimens were kept in 100% methanol at –20 °C before use.

Riboprobes for *in situ* hybridization

The *in situ* hybridization was performed using the P1 riboprobe which was an 808bp PCR fragment targeted to the 3' end of *Lrp4* coding region (from 4921bp to 5728bp, Fig. 4B), *L-Ipo13*-specific L-probe and C-probe which recognizes both *L-Ipo13* and *TS-Ipo13* transcripts (Fig. 10) and riboprobes of 1.3 kb full-length cDNA for detection of *Pou5f1* (*Oct-3/4*) cDNA (gift from Prof. H. Hamada) and a 503 bp cDNA spanning in ORF of germ-cell-specific *Ddx4* (*Mvh*) (Fujiwara et al., 1994).

Whole-mount *in situ* hybridization

Procedure for *in situ* hybridization was described by Wilkinson (1992). In brief, tissue specimens were incubated with the digoxygenin-labeled probe (Roche) in 50% formamide hybridization buffer at 70C° for at least 16 hours. After the washing with tris-buffered serine tween (TBST), the digoxygenin-labeled probe was detected by alkaline phosphatase-conjugated anti-digoxygenin antibody according to the manufacture's instruction (Roche).

Fluorescence double whole-mount *in situ* hybridization

Fluorescence double whole-mount *in situ* hybridization was performed as described by Tanaka and Matsui (2002) using digoxygenin-labeled probe for either *Lrp4* or *Ipo13*, and biotin-labeled probe for *Pou5f1* (*Oct-3/4)* probe (Roche). The dorsal mesentery and slices of the trunk of E9.5 embryo, the genital ridge of E10.5 and E11.5 embryos, and the gonads of E13.5 embryo were dissected. The digoxygenin-or biotin-labeled probe was detected by FITC conjugated anti-digoxygenin antibody or Rhodamine complexed strept avidin according to the manufacture's instruction (Roche), respectively. Fluorescence images were captured by Leica DMRB/E and Leica SP2 confocal scanning system.

Section *in situ* hybridization

Procedures for the section *in situ* hybridization are according to the methods in Saijoh *et al.* (1996). The specimens were incubated with digoxigenin–labeled probe for *Lrp4*, or both digoxigenin–labeled probe for *Ipo13* and biotin-labeled riboprobe for *Ddx4* in 50%

formamide hybridization buffer at 55C° for 40 hours. Fluorescence imaging was performed using an Olympus BX51 microscope and digital images were recorded using Olympus DP-11 camera.

Immunohistochemisry

Immunostaining of DDX4 in fetal gonads was done with anti-DDX4 antibody (1:5000) (gift from Dr. T. Noce; Toyooka et al., 2000) and Alexa488-tagged anti-rabbit secondary antibody (1:1000; Molecular Probe). Anti-TRA98 antibody staining in newborn and adult testes was done with anti-TRA98 serum (1:5)(gift from Prof. Y. Nishimune; Tanaka et al., 1997) and Alexa350-tagged anti-rat secondary antibody (1:1000; Molecular Probe). Fluorescence imaging was performed using an Olympus BX51 microscope and Olympus DP-11 camera system.

For the immunostaining of UBC9 in the germ cells, 10 μm paraffin sections of adult testis and fetal ovary were incubated with retrieval solution according to the manufacturer's instructions (pH 6.0, DAKO). After treatment with 0.3% Boheringer blocking reagent (BBR; Roche), sections were incubated with 1/250 dilution of anti-UBC9 mouse monoclonal antibody (Pharmingen) in 0.1% BBR at 4°C for 16 hours. Detection was done by ABC staining kit according to manufacture's instructions (Vectastain). The images were recorded using Nikon OPTIPHOT-2 microscope and SPOT camera with SPOT advanced version 4.0.1 acquisition soft ware (Diagnostic Instruments Inc, USA).

For immunostaining of germ cells in cultured and intact fetal ovaries, the specimens were fixed with 4% PFA and embedded in OCT compound (Tissue-Tek). Frozen 10 μm-thick sections were prepared by Cryostat, and treated with 1/200 dilution of anti-SCP3 rabbit monoclonal antibody (gift from Prof. N. Nakatsuiji; Chuma and Nakatsuji, 2001). The sections were then treated with Alexa594-tagged anti-rabbit secondary antibody at 1/1000 dilution (Molecular Probe), followed by DAPI (SIGMA) staining. Immunostaining of Myc-tagged fusion-protein was done using anti-MYC antibody at 1/250 dilution (SIGMA) and Alexa594-tagged anti-mouse secondary antibody at 1/750 dilution (Molecular Probe). Fluorescence imaging was performed using an Olympus BX51 microscope and Olympus DP-11 camera system.

Enforced expression of IPO13 in GC1 cells

Expression vectors compromising of a CMV-promoter and an IRES-EGFP expression vector

(*pIRES-EGFP*; Clontech; also used as a control vector) into which sequences coding for full size IPO13 protein (*pCMV-L-Ipo13-FLAG-IRES-EGFP*) or the short isoform of IPO13 (*pCMV-TS-Ipo13-FLAG-IRES-EGFP*) were incorporated. Open reading frames of either *L-Ipo13* or *TS-Ipo13* were amplified by RT-PCR and fused in frame to a FLAG-tag at the C-terminal end, then inserted into the multi-cloning site of *pIRES-EGFP*. Construction of *pCI-Ubc9-Myc* expression vector was described by Machon et al. (2000). GC1 cells were cultured in DMEM containing 10% FCS on a four well chamber slide (NUNC). Expression vectors of IPO13 and UBC9 were lipofected using Lipofect-amine 2000 transfection reagent (QIAGEN), according to manufacture's instructions. About 6 hours after transfection at 37°C, cells were fixed with 4% PFA to examine the distribution of UBC9-MYC fusion-protein in the cells.

Western Blot

Western blot analysis was performed by using the anti-IPO13 rabbit antibody against IPO13 peptides (RERVNKRRVKEMVK, Hokkaido System Science Co.). Both anti-IPO13 and anti-FLAG antibodies detected a same 92kDa band in pCMV-IPO13-FLAG-IRES-eGFP lipofected STO cells (data not shown). For Western blot analysis, the detection of IPO13 protein either in adult testis (about 10000 cells per lane) or in fetal ovary (1 ovary per lane) was done by using anti-IPO13 primary antibodies (1:500) and horseradish peroxidase conjugated secondary antibody (1:10000; Bio-Rad) according to manufacturer's instructions. An additional 40kDa band for predicted TS-IPO13 was detected using with anti-IPO13 antibody in the adult testis.

***In vitro* culture and siRNA treatment of the fetal ovary**

Results of a preliminary study on the efficiency of introducing EGFP expression construct by lipofection showed that a more consistent outcome was achieved in fetal ovary than neonatal testes. The experiment of down-regulation of *L-Ipo13* activity on the progression of meiosis was therefore performed on the E15.5 fetal ovary. E15.5 ovaries were sliced open and immersed for 4 minutes in a liposome solution containing one of the three siRNA reagents: siRNA#1, siRNA#2 or scrambled sequence (QIAGEN) prepared as per RNAiFect methods (QIAGEN). The sequence of the siRNA construct and the targeted *Ipo13* sequences are: siRNA#1: ccgaccagtatgaaagcttaa targeted to 913-933bp (NM_146152), siRNA#2: cacggactacacagctgacta to 3497-3517bp (NM_146152), and scrambled sequence control:

aattctccgaacgtgtcacgt. The 3' end of the sense sequence of each construct was tagged with Alexa488 green Fluorescent dye (QIAGEN).

The treated ovaries were cultured for 3 days on 0.3 μm of isopore membrane filters (Millipore) floating on DMEM with 20% FCS in 5% CO_2 in air at 37°C (Park and Taketo, 2003). The efficiency of *Ipo13* knockdown was assessed by Western blot and RT-PCR analysis.

Generation of cDNA pools

cDNAs were synthesized and were amplified by PCR according to the method by Shimono and Behringer (1999). In brief, about fifty cells of dissected proximal epiblast and distal epiblast of the E6.25 embryo were lysed by heat treatment at 65°C and first-strand cDNA was synthesized using a mixture of moloney murine leukemia virus (Gibco/BRL) and avian myeloblastosis virus reverse transcriptase (Roche) with poly-d(T) primer at 37°C for 15 min. Poly-d(A) was added onto 3' end of the first-strand cDNA by terminal transferase (Roche) at 37°C for 15 min and then amplified by PCR with poly-d(T) containing primer.

Subtraction

The subtraction procedure was also according to the method of Shimono and Behringer (1999). PCR-based subtraction was carried out 3 times to generate a proximal epiblast-specific subtracted cDNA library. Amplified cDNA pools were electrophoresed and were used for Southern blot analysis to monitor the subtraction efficiencies after each subtraction step. After subtraction, the cDNA fragments were ligated into plasmid vectors (pBluescript or pGemT Easy), which were further screened to obtain proximal epiblast-specific genes.

Screening of candidate clones by Southern blot hybridization

1st screening 500 clones from the 2nd subtracted library were screened by Southern blot hybridization using three probes: unsubtracted proximal and distal epiblast cDNAs and cDNAs after the 3rd subtraction. For the hybridization, the membrane was incubated with the ^{32}P-labeled probe in hybridization buffer at 65°C for 16 hours, and the membrane was washed in 0.2% X SSC containing 0.1% SDS at 65°C for 20 minutes twice. 23 clones showed the specific hybridization pattern with proximal probes.

2nd screening To further verify whether the positive clones were specifically expressed in proximal epiblast, positive clones were used as probes for Southern blots of cDNA pools of

proximal epiblast and distal epiblast. 8 clones showed the specific hybridization pattern in the proximal epiblast cDNA pool significantly.

REFERENCES

Anderson, R., Copeland, T. K., Scholer, H., Heasman, J., and Wylie, C. (2000). The onset of germ cell migration in the mouse embryo. *Mech Dev* **91,** 61-8.

Andra, K., Lassmann, H., Bittner, R., Shorny, S., Fassler, R., Propst, F., and Wiche, G. (1997). Targeted inactivation of plectin reveals essential function in maintaining the integrity of skin, muscle, and heart cytoarchitecture. *Genes Dev* **11,** 3143-56.

Anway, M. D., Li, Y., Ravindranath, N., Dym, M., and Griswold, M. D. (2003). Expression of testicular germ cell genes identified by differential display analysis. *J Androl* **24,** 173-84.

Apionishev, S., Malhotra, D., Raghavachari, S., Tanda, S., and Rasooly, R. S. (2001). The Drosophila UBC9 homologue lesswright mediates the disjunction of homologues in meiosis I. *Genes Cells* **6,** 215-24.

Boswell, R. E., Prout, M. E., and Steichen, J. C. (1991). Mutations in a newly identified Drosophila melanogaster gene, mago nashi, disrupt germ cell formation and result in the formation of mirror-image symmetrical double abdomen embryos. *Development* **113,** 373-84.

Chambers, I., Colby, D., Robertson, M., Nichols, J., Lee, S., Tweedie, S., and Smith, A. (2003). Functional expression cloning of Nanog, a pluripotency sustaining factor in embryonic stem cells. *Cell* **113,** 643-55.

Chuma, S., and Nakatsuji, N. (2001). Autonomous transition into meiosis of mouse fetal germ cells in vitro and its inhibition by gp130-mediated signaling. *Dev Biol* **229,** 468-79.

de Sousa Lopes, S. M., Roelen, B. A., Monteiro, R. M., Emmens, R., Lin, H. Y., Li, E., Lawson, K. A., and Mummery, C. L. (2004). BMP signaling mediated by ALK2 in the visceral endoderm is necessary for the generation of primordial germ cells in the mouse embryo. *Genes Dev* **18,** 1838-49.

Eddy, E. M. (1975). Germ plasm and the differentiation of the germ cell line. *Int Rev Cytol* **43,**

229-80.

FANTOM Consortium (2002). Analysis of the mouse transcriptome based on functional annotation of 60,770 full-length cDNAs. *Nature* **420**,563-573.

Fujiwara, Y., Komiya, T., Kawabata, H., Sato, M., Fujimoto, H., Furusawa, M., and Noce, T. (1994). Isolation of a DEAD-family protein gene that encodes a murine homolog of Drosophila vasa and its specific expression in germ cell lineage. *Proc Natl Acad Sci U S A* **91,** 12258-62.

Geles, K. G., and Adam, S. A. (2001). Germline and developmental roles of the nuclear transport factor importin alpha3 in C. elegans. *Development* **128,** 1817-30.

Giarre, M., Torok, I., Schmitt, R., Gorjanacz, M., Kiss, I., and Mechler, B. M. (2002). Patterns of importin-alpha expression during Drosophila spermatogenesis. *J Struct Biol* **140,** 279-90.

Ginsburg, M., Snow, M. H., and McLaren, A. (1990). Primordial germ cells in the mouse embryo during gastrulation. *Development* **110,** 521-8.

Gorjanacz, M., Adam, G., Torok, I., Mechler, B. M., Szlanka, T., and Kiss, I. (2002). Importin-alpha 2 is critically required for the assembly of ring canals during Drosophila oogenesis. *Dev Biol* **251,** 271-82.

Herz, J., and Bock, H. H. (2002). Lipoprotein receptors in the nervous system. *Annu Rev Biochem* **71,** 405-34.

Herz, J., Clouthier, D. E., and Hammer, R. E. (1992). LDL receptor-related protein internalizes and degrades uPA-PAI-1 complexes and is essential for embryo implantation. *Cell* **71,** 411-21.

Hey, P. J., Twells, R. C., Phillips, M. S., Yusuke, N., Brown, S. D., Kawaguchi, Y., Cox, R., Guochun, X., Dugan, V., Hammond, H., Metzker, M. L., Todd, J. A., and Hess, J. F. (1998). Cloning of a novel member of the low-density lipoprotein receptor family. *Gene* **216,** 103-11.

Hofmann, M. C., Narisawa, S., Hess, R. A., and Millan, J. L. (1992). Immortalization of germ cells and somatic testicular cells using the SV40 large T antigen. *Exp Cell Res* **201,** 417-35.

Hogarth, C., Itman, C., Jans, D. A., and Loveland, K. L. (2005). Regulated nucleocytoplasmic transport in spermatogenesis: a driver of cellular differentiation? *Bioessays* **27,** 1011-25.

Johnson, E. B., Hammer, R. E., and Herz, J. (2005). Abnormal development of the apical ectodermal ridge and polysyndactyly in Megf7-deficient mice. *Hum Mol Genet* **14,** 3523-38.

Kahle, J., Baake, M., Doenecke, D., and Albig, W. (2005). Subunits of the heterotrimeric transcription factor NF-Y are imported into the nucleus by distinct pathways involving importin beta and importin 13. *Mol Cell Biol* **25,** 5339-54.

Kimura, T., Suzuki, A., Fujita, Y., Yomogida, K., Lomeli, H., Asada, N., Ikeuchi, M., Nagy, A., Mak, T. W., and Nakano, T. (2003). Conditional loss of PTEN leads to testicular teratoma and enhances embryonic germ cell production. *Development* **130,** 1691-700.

Kimura, T., Nakamura, T., Murayama, K., Umehara, H., Yamano, N., Watanabe, S., Taketo, M. M., and Nakano T. (in press) The stabilization of β-catenin leads to impaired primordial germ cell development via aberrant cell cycle progression. Dev Biol, doi:10.1016/j.ydbio.2006.06.038

Kovalenko, O. V., Plug, A. W., Haaf, T., Gonda, D. K., Ashley, T., Ward, D. C., Radding, C. M., and Golub, E. I. (1996). Mammalian ubiquitin-conjugating enzyme Ubc9 interacts with Rad51 recombination protein and localizes in synaptonemal complexes. *Proc Natl Acad Sci U S A* **93,** 2958-63.

Labosky, P. A., Barlow, D. P., and Hogan, B. L. (1994). Mouse embryonic germ (EG) cell lines: transmission through the germline and differences in the methylation imprint of insulin-like growth factor 2 receptor (Igf2r) gene compared with embryonic stem (ES) cell lines. *Development* **120,** 3197-204.

Lange, U. C., Saitou, M., Western, P. S., Barton, S. C., and Surani, M. A. (2003). The fragilis interferon-inducible gene family of transmembrane proteins is associated with germ cell specification in mice. *BMC Dev Biol* **3,** 1.

Lawson, K. A., and Hage, W. J. (1994). Clonal analysis of the origin of primordial germ cells in the mouse. *Ciba Found Symp* **182,** 68-84.

Lawson, K. A., Dunn, N. R., Roelen, B. A., Zeinstra, L. M., Davis, A. M., Wright, C. V., Korving, J. P., and Hogan, B. L. (1999). Bmp4 is required for the generation of primordial germ cells in the mouse embryo. *Genes Dev* **13,** 424-36.

Leatherman, J. L., and Jongens, T. A. (2003). Transcriptional silencing and translational control: key features of early germline development. *Bioessays* **25,** 326-35.

Lickert, H., Cox, B., Wehrle, C., Taketo, M. M., Kemler, R., and Rossant, J. (2005). Dissecting Wnt/beta-catenin signaling during gastrulation using RNA interference in mouse embryos. *Development* **132,** 2599-609.

Lin, Y., and Page, D. C. (2005). Dazl deficiency leads to embryonic arrest of germ cell development in XY C57BL/6 mice. *Dev Biol* **288,** 309-16.

Lopez-Casas, P. P., Lopez-Fernandez, L. A., Parraga, M., Krimer, D. B., and del Mazo, J. (2003). Developmental regulation of expression of Ran/M1 and Ran/M2 isoforms of Ran-GTPase in mouse testis. *Int J Dev Biol* **47,** 307-10.

Loveland, K. L., Hogarth, C., Szczepny, A., Prabhu, S. M., and Jans, D. A. (2005). Expression of Nuclear Transport Importins beta 1 and beta 3 Is Regulated During Rodent Spermatogenesis. *Biol Reprod.*

MacGregor, G. R., Zambrowicz, B. P., and Soriano, P. (1995). Tissue non-specific alkaline phosphatase is expressed in both embryonic and extraembryonic lineages during mouse embryogenesis but is not required for migration of primordial germ cells. *Development* **121,** 1487-96.

Machon, O., Backman, M., Julin, K., and Krauss, S. (2000). Yeast two-hybrid system identifies the ubiquitin-conjugating enzyme mUbc9 as a potential partner of mouse Dac. *Mech Dev* **97,** 3-12.

Mason, D. A., Fleming, R. J., and Goldfarb, D. S. (2002). Drosophila melanogaster importin alpha1 and alpha3 can replace importin alpha2 during spermatogenesis but not oogenesis. *Genetics* **161,** 157-70.

Matsui, Y., and Okamura, D. (2005). Mechanisms of germ-cell specification in mouse embryos. *Bioessays* **27,** 136-43.

McClellan, K. A., Gosden, R., and Taketo, T. (2003). Continuous loss of oocytes throughout meiotic prophase in the normal mouse ovary. *Dev Biol* **258,** 334-48.

McLaren, A. (2003). Primordial germ cells in the mouse. *Dev Biol* **262,** 1-15.

McLaren, A., and Lawson, K. A. (2005). How is the mouse germ-cell lineage established? *Differentiation* **73,** 435-7.

Melchior, F. (2000). SUMO--nonclassical ubiquitin. *Annu Rev Cell Dev Biol* **16,** 591-626.

Mingot, J. M., Kostka, S., Kraft, R., Hartmann, E., and Gorlich, D. (2001). Importin 13: a novel mediator of nuclear import and export. *Embo J* **20,** 3685-94.

Mitsui, K., Tokuzawa, Y., Itoh, H., Segawa, K., Murakami, M., Takahashi, K., Maruyama, M., Maeda, M., and Yamanaka, S. (2003). The homeoprotein Nanog is required for maintenance of pluripotency in mouse epiblast and ES cells. *Cell* **113,** 631-42.

Molyneaux, K., and Wylie, C. (2004). Primordial germ cell migration. *Int J Dev Biol* **48,** 537-44.

Nacerddine, K., Lehembre, F., Bhaumik, M., Artus, J., Cohen-Tannoudji, M., Babinet, C.,

Pandolfi, P. P., and Dejean, A. (2005). The SUMO pathway is essential for nuclear integrity and chromosome segregation in mice. *Dev Cell* **9,** 769-79.

Nakayama, M., Nakajima, D., Nagase, T., Nomura, N., Seki, N., and Ohara, O. (1998). Identification of high-molecular-weight proteins with multiple EGF-like motifs by motif-trap screening. *Genomics* **51,** 27-34.

Nichols, J., Zevnik, B., Anastassiadis, K., Niwa, H., Klewe-Nebenius, D., Chambers, I., Scholer, H., and Smith, A. (1998). Formation of pluripotent stem cells in the mammalian embryo depends on the POU transcription factor Oct4. *Cell* **95,** 379-91.

Nonn, L., Williams, R. R., Erickson, R. P., and Powis, G. (2003). The absence of mitochondrial thioredoxin 2 causes massive apoptosis, exencephaly, and early embryonic lethality in homozygous mice. *Mol Cell Biol* **23,** 916-22.

Nykjaer, A., and Willnow, T. E. (2002). The low-density lipoprotein receptor gene family: a cellular Swiss army knife? *Trends Cell Biol* **12,** 273-80.

Ohinata, Y., Payer, B., O'Carroll, D., Ancelin, K., Ono, Y., Sano, M., Barton, S. C., Obukhanych, T., Nussenzweig, M., Tarakhovsky, A., Saitou, M., and Surani, M. A. (2005). Blimp1 is a critical determinant of the germ cell lineage in mice. *Nature* **436,** 207-13.

Ohta, H., Tohda, A., and Nishimune, Y. (2003). Proliferation and differentiation of spermatogonial stem cells in the w/wv mutant mouse testis. *Biol Reprod* **69,** 1815-21.
Park, E. H., and Taketo, T. (2003). Onset and progress of meiotic prophase in the oocytes in the B6.YTIR sex-reversed mouse ovary. *Biol Reprod* **69,** 1879-89.

Park, E. H., and Taketo, T. (2003). Onset and progress of meiotic prophase in the oocytes in the B6.YTIR sex-reversed mouse ovary. *Biol Reprod* **69,** 1879-89.

Payer, B., Saitou, M., Barton, S. C., Thresher, R., Dixon, J. P., Zahn, D., Colledge, W. H., Carlton, M. B., Nakano, T., and Surani, M. A. (2003). Stella is a maternal effect gene required for normal early development in mice. *Curr Biol* **13,** 2110-7.

Pepling, M. E., and Spradling, A. C. (2001). Mouse ovarian germ cell cysts undergo programmed breakdown to form primordial follicles. *Dev Biol* **234,** 339-51.

Pesce, M., Gross, M. K., and Scholer, H. R. (1998). In line with our ancestors: Oct-4 and the mammalian germ. *Bioessays* **20,** 722-32.

Pinson, K. I., Brennan, J., Monkley, S., Avery, B. J., and Skarnes, W. C. (2000). An LDL-receptor-related protein mediates Wnt signalling in mice. *Nature* **407,** 535-8.

Plafker, S. M., Plafker, K. S., Weissman, A. M., and Macara, I. G. (2004). Ubiquitin charging of human class III ubiquitin-conjugating enzymes triggers their nuclear import. *J Cell Biol* **167,** 649-59.

Ploski, J. E., Shamsher, M. K., and Radu, A. (2004). Paired-type homeodomain transcription factors are imported into the nucleus by karyopherin 13. *Mol Cell Biol* **24,** 4824-34.

Rongo, C., and Lehmann, R. (1996). Regulated synthesis, transport and assembly of the Drosophila germ plasm. *Trends Genet* **12,** 102-9.

Russell, L.D., Ettlin, R.A., Sinha Hikim, A.P., Clegg, E.D., 1990. Staging for laboratory species. In: Russell, L.D., Ettlin, R.A., Sinha Hikim, A.P., Clegg, E.D. (Eds), Histological and Histopathological Evalutation of the Testis, Cache River Press., Clearwater, pp. 119-161.

Saijoh, Y., Fujii, H., Meno, C., Sato, M., Hirota, Y., Nagamatsu, S., Ikeda, M., and Hamada, H. (1996). Identification of putative downstream genes of Oct-3, a pluripotent cell-specific transcription factor. *Genes Cells* **1,** 239-52.

Saitou, M., Barton, S. C., and Surani, M. A. (2002). A molecular programme for the specification of germ cell fate in mice. *Nature* **418,** 293-300.

Sato, M., Kimura, T., Kurokawa, K., Fujita, Y., Abe, K., Masuhara, M., Yasunaga, T., Ryo, A., Yamamoto, M., and Nakano, T. (2002). Identification of PGC7, a new gene expressed

specifically in preimplantation embryos and germ cells. *Mech Dev* **113,** 91-4.

Sato, N., Meijer, L., Skaltsounis, L., Greengard, P., and Brivanlou, A. H. (2004). Maintenance of pluripotency in human and mouse embryonic stem cells through activation of Wnt signaling by a pharmacological GSK-3-specific inhibitor. *Nat Med* **10,** 55-63.

Schalk, J. A., Dietrich, A. J., Vink, A. C., Offenberg, H. H., van Aalderen, M., and Heyting, C. (1998). Localization of SCP2 and SCP3 protein molecules within synaptonemal complexes of the rat. *Chromosoma* **107,** 540-8.

Seeler, J. S., and Dejean, A. (2003). Nuclear and unclear functions of SUMO. *Nat Rev Mol Cell Biol* **4,** 690-9.

Shimono, A., and Behringer, R. R. (1999). Isolation of novel cDNAs by subtractions between the anterior mesendoderm of single mouse gastrula stage embryos. *Dev Biol* **209,** 369-80.

Simon-Chazottes D.C., Tutois S., Bourgade F., Evans M., Kuehn M. and Guenet J.-L., 2000. Characteization of an insertional mutation responsible for abnormal limb develompent. NCBI Protein locus entry AAL36970.

Strom, A. C., and Weis, K. (2001). Importin-beta-like nuclear transport receptors. *Genome Biol* **2,** REVIEWS3008.

Tam, P. P., and Zhou, S. X. (1996). The allocation of epiblast cells to ectodermal and germ-line lineages is influenced by the position of the cells in the gastrulating mouse embryo. *Dev Biol* **178,** 124-32.

Tanaka, H., Pereira, L. A., Nozaki, M., Tsuchida, J., Sawada, K., Mori, H., and Nishimune, Y. (1997). A germ cell-specific nuclear antigen recognized by a monoclonal antibody raised against mouse testicular germ cells. *Int J Androl* **20,** 361-6.

Tanaka, S. S., Toyooka, Y., Akasu, R., Katoh-Fukui, Y., Nakahara, Y., Suzuki, R., Yokoyama, M., and Noce, T. (2000). The mouse homolog of Drosophila Vasa is required for the

development of male germ cells. *Genes Dev* **14,** 841-53.

Tanaka, S. S., and Matsui, Y. (2002). Developmentally regulated expression of mil-1 and mil-2, mouse interferon-induced transmembrane protein like genes, during formation and differentiation of primordial germ cells. *Mech Dev* **119 Suppl 1,** S261-7.

Tanaka, S. S., Nagamatsu, G., Tokitake, Y., Kasa, M., Tam, P. P., and Matsui, Y. (2004). Regulation of expression of mouse interferon-induced transmembrane protein like gene-3, Ifitm3 (mil-1, fragilis), in germ cells. *Dev Dyn* **230,** 651-9.

Tanaka, S. S., Yamaguchi, Y. L., Tsoi, B., Lickert, H., and Tam, P. P. (2005). IFITM/Mil/fragilis family proteins IFITM1 and IFITM3 play distinct roles in mouse primordial germ cell homing and repulsion. *Dev Cell* **9,** 745-56.

Tanaka, T., Hosoi, F., Yamaguchi-Iwai, Y., Nakamura, H., Masutani, H., Ueda, S., Nishiyama, A., Takeda, S., Wada, H., Spyrou, G., and Yodoi, J. (2002). Thioredoxin-2 (TRX-2) is an essential gene regulating mitochondria-dependent apoptosis. *Embo J* **21,** 1695-703.

Tao, T., Lan, J., Presley, J. F., Sweezey, N. B., and Kaplan, F. (2004). Nucleocytoplasmic shuttling of lgl2 is developmentally regulated in fetal lung. *Am J Respir Cell Mol Biol* **30,** 350-9.

Toyooka, Y., Tsunekawa, N., Takahashi, Y., Matsui, Y., Satoh, M., and Noce, T. (2000). Expression and intracellular localization of mouse Vasa-homologue protein during germ cell development. *Mech Dev* **93,** 139-49.

Vainio, S., Heikkila, M., Kispert, A., Chin, N., and McMahon, A. P. (1999). Female development in mammals is regulated by Wnt-4 signalling. *Nature* **397,** 405-9.

Vincent, S. D., Dunn, N. R., Sciammas, R., Shapiro-Shalef, M., Davis, M. M., Calame, K., Bikoff, E. K., and Robertson, E. J. (2005). The zinc finger transcriptional repressor Blimp1/Prdm1 is dispensable for early axis formation but is required for specification of primordial germ cells in the mouse. *Development* **132,** 1315-25.

Weis, K. (2002). Nucleocytoplasmic transport: cargo trafficking across the border. *Curr Opin Cell Biol* **14,** 328-35.

Weis, K. (2003). Regulating access to the genome: nucleocytoplasmic transport throughout the cell cycle. *Cell* **112,** 441-51.

Wiche, G. (1998). Role of plectin in cytoskeleton organization and dynamics. *J Cell Sci* **111 (Pt 17),** 2477-86.

Wilkinson, D.G. (Ed), 1992. In situ hybridization: A practical approach, Oxford university press, New York.

Wylie, C. (1999). Germ cells. *Cell* **96,** 165-74.

Yamaguchi, S., Kimura, H., Tada, M., Nakatsuji, N., and Tada, T. (2005). Nanog expression in mouse germ cell development. *Gene Expr Patterns* **5,** 639-46.

Yeom, Y. I., Fuhrmann, G., Ovitt, C. E., Brehm, A., Ohbo, K., Gross, M., Hubner, K., and Scholer, H. R. (1996). Germline regulatory element of Oct-4 specific for the totipotent cycle of embryonal cells. *Development* **122,** 881-94.

Yoneda, Y. (2000). Nucleocytoplasmic protein traffic and its significance to cell function. *Genes Cells* **5,** 777-87.

Yoshimizu, T., Obinata, M., and Matsui, Y. (2001). Stage-specific tissue and cell interactions play key roles in mouse germ cell specification. *Development* **128,** 481-90.

Zhang, C., Sweezey, N. B., Gagnon, S., Muskat, B., Koehler, D., Post, M., and Kaplan, F. (2000). A novel karyopherin-beta homolog is developmentally and hormonally regulated in fetal lung. *Am J Respir Cell Mol Biol* **22,** 451-9.

Zhao, G. Q., and Garbers, D. L. (2002). Male germ cell specification and differentiation. *Dev*

Cell **2,** 537-47.

Zhao, X. F., Colaizzo-Anas, T., Nowak, N. J., Shows, T. B., Elliott, R. W., and Aplan, P. D. (1998). The mammalian homologue of mago nashi encodes a serum-inducible protein. *Genomics* **47,** 319-22.

ACKNOWLEDGEMENTS

I would like to express my sincere to indebtedness to Prof. Patrick P. L. Tam, supervisor of my study, and Prof. Kunio Yasuda for their patient guidance throughout my course of study and help extended to me in preparing this thesis. I appreciate the very kind help in preparing this thesis by Prof. Yoshiko Takahashi. I would like to thank Prof. Y. Matsui and his laboratory members and all the member of research institute, Osaka Medical Center for Maternal and Child Health.

I deeply appreciate the very kind help, stimulative discussion and cooking offered by Dr Satomi S. Tanaka in the laboratory and home during the course of my study and preparing this thesis.

I am grateful for Drs. David Loebel and Samara Lewis, Renuka Rao, Gregory Pelka and Mrs. Kirsten Steiner, Poh-Lynn Khoo, Melinda Hayward, Bonny Tsoi, Nichole Wong, and all the member of Embryology unit of Children's Medical Research Institute for their very kind help and stimulative discussion.

I wish to thank Drs. Norio Nakatsuji for anti-SCP3 antibody, Stefan Krauss for pCI-*Ubc9*-Myc expression construct, Yukio Saijho for his technical advice, Hiroshi Hamada for *Pou5f1* probe, Toshiaki Noce for anti-DDX4 antibody, Yoshitake Nishimune for anti-TRA98 antibody and Noriyuki Sugiyama for W/W^v mutant mouse testis cDNA, Hiroko Toyoda-Ohno for the RNA preparations of ES and EG cells, and Kate Loveland for the GC1 cell line.

At the end, I would like to express my sincere sense of heart-felt gratitude to my parents and sister, so warmly supported me throughout course of my study.

ABSTRACT (in Japanese)

生殖細胞は遺伝情報を次世代に伝えるために特殊化した細胞であり、減数分裂をへて、配偶子へと分化する。また、マウスの生殖系列細胞は、培養下において pluripotent cell lines へと移行する能力を秘めた唯一の細胞系譜である。マウスの生殖細胞の運命決定には、他の動物種で示されているような卵子中に蓄積されている母性効果因子群に依存せず、原始外胚葉の上端部に位置する細胞と周囲の組織との相互作用により誘導されると考えられる。マウスの生殖細胞は、アルカリフォスファターゼ(Tissue non-specific alkaline phosphatase: TNAP)活性強陽性の始原生殖細胞（primordial germ cells: PGCs）として初めて組織学的に検出される。しかし、TNAP を含めた PGCs 特異的に発現する分子群は、inner cell mass (ICM)や ES 細胞、EG 細胞といった pluripotent cell lines にも発現しており、これらの多能性幹細胞と生殖細胞との違いを担う分子基盤についてはほとんど知られていない。そこで、PGCs と ICM を含む blastocyst との間のサブトラクティブ cDNA スクリーニングをおこない、PGCs に特異的に発現し、生殖細胞の特性を担うと考えられる５つの候補遺伝子が同定された(Tanaka and Matsui, Mech. Dev. 119S, S261-267, 2002)。得られた候補遺伝子群について、生殖細胞の発生・分化過程におけるその役割を調べていくことは、マウス生殖細胞が、生殖細胞としての特性を獲得して次世代に遺伝情報を伝えるために配偶子へと分化していく分子機構の解明につながると考えられる。

本論文では、１）マウス生殖細胞の分化、および EG 細胞の形成過程に関わることが推測される候補遺伝子、Low density lipoprotein receptor-related protein 4 (*Lrp4*)と、２）減数分裂の制御に関わることが推測される候補遺伝子、*Importin13* (*Ipo13*)の２つの候補遺伝子に着目し、その解析について述べている。

Lrp4 は、発生初期の PGCs においては観察されず、胎仔生殖巣に到達する頃の PGCs からその高発現が観察される。生殖巣内の生殖細胞での *Lrp4* の発現は、雌では未成熟な卵子、雄では精粗細胞まで引き続き観察された。一方、*Lrp4* の発現は、ICM や原始外胚葉、また ES 細胞や EG 細胞といった多能性幹細胞には発現が認められなかった。LRP4 は、Wnt-signaling の co-receptor として働く LRP5 や LRP6 と比較して、シグナル伝達に必要な細胞内領域の構造が異なることから推測されていた通り、LRP5 および LRP6 に対してドミナントネガティブに働き、Wnt-signaling を遮断する働きがあることが近年報告された。一方、Wnt-signaling は ES 細胞の自己増殖に重要な役割を果たしていることが知られており、PGCs における *Lrp4* 遺伝子活性の上昇は、PGCs の増殖や分化に関わっている可能性が考えられる。また、PGCs からの EG

細胞の樹立においても、この *Lrp4* 遺伝子の発現低下が重要な働きを担っていることが推測される。

もう１つの候補遺伝子である *Ipo13* は、細胞質核間の物質輸送を担う Importin-βファミリーに属し、移動期および生殖巣に定着した PGCs において特異的な発現が観察された。マウスにおいて *Ipo13* 転写産物の発現を調べたところ、二種類の転写産物、*L-Ipo13* と精巣でのみに発現する short-isoform の *TS-Ipo13* が存在した。

生殖巣での *Ipo13* の発現についてその発生過程を追って調べた結果、*L-Ipo13* は雌雄ともに減数分裂過程のパキテン期の生殖細胞に強く発現しており、一方、*TS-Ipo13* は、４週齢以降の精巣の生殖細胞においてのみ発現していた。*L-Ipo13* 遺伝子活性は、ヒト IPO13 タンパク質が輸送する cargo の１つである ubiquitin binding complex 9(UBC9)の核への局在化を促進したが、*TS-Ipo13* 遺伝子活性は、UBC9 の核への局在化を誘導しなかった。また、*TS-Ipo13* を *L-Ipo13* と共発現させると、UBC9-MYC の核への局在が阻害されることから、TS-IPO13 が、L-IPO13 の核への物質輸送活性に対して negative regulator として働くことが示唆された。一方、培養胎仔卵巣を用いた siRNA による *Ipo13* のジーンサイレンシングの実験より、*L-Ipo13* 遺伝子産物の発現低下が、UBC9 の核への局在が阻害されること、そしてパキテン後期へと分化した生殖細胞の細胞数の減少を引き起こすことから、雌の生殖細胞の減数分裂の進行に重要な働きを担っていることが明らかとなった。また、精巣の精母細胞での UBC9 の核への局在化は、*L-Ipo13* のパキテン期特異的な発現の後に起こることが観察されたことからも、*Ipo13* の生殖細胞での時期特異的な高発現が、減数分裂の進行において重要な役割を果たすと考えられる分子群の細胞内局在を変化させ、細胞分化を起こすトリガーになっていると考えられる。

以上の研究から、マウス生殖細胞が、生殖細胞としての特性を獲得して分化していく過程、特に減数分裂過程での生殖細胞の分化を制御している分子機構の一端を明らかにした。細胞内局在の変化が、その分子の機能を制御しているいくつかの例は知られているが、その細胞内局在の変化の時期特異的な制御機構については、未だよく知られていない。また、TS-IPO13 による L-IPO13 の細胞間物質輸送活性の制御機構のモデルは、これまで知られていなかった Importin の分子機能の制御機構として非常に興味深い。生殖細胞での IPO13 の cargo 分子の同定と IPO13 の細胞間物質輸送の活性制御機構機を解明していくことは、今後、細胞分化を制御する分子機構を理解していく上で、重要な糸口の１つであると考えられる。